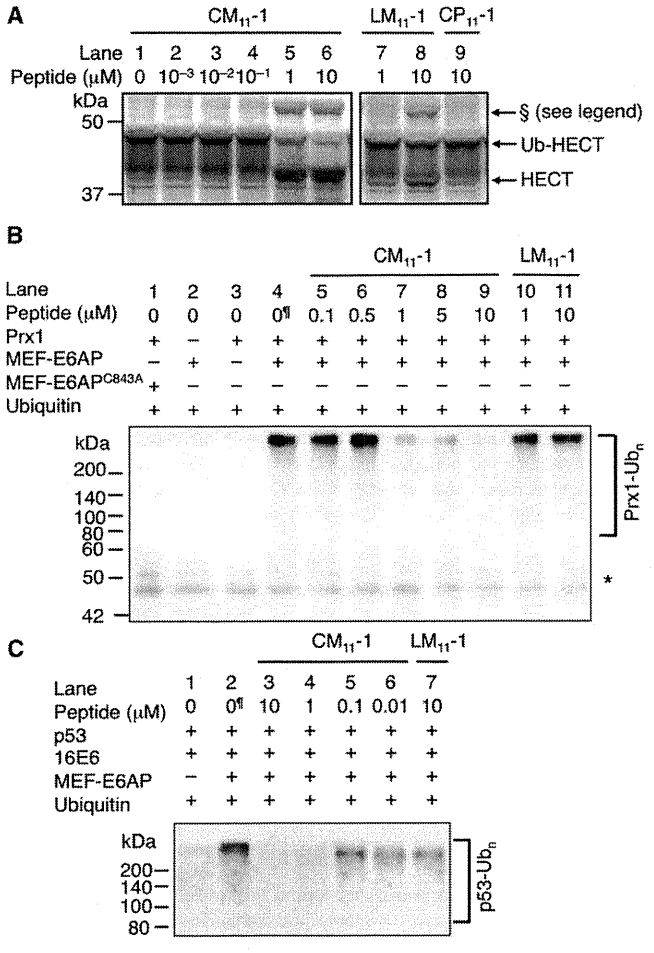

Figure 4. Inhibition of Ub-Thioester Formation with E6AP HECT Domain and Polyubiqutination of Target Proteins by CM_{11}-1 and Its Derivatives

(A) Inhibition of Ub-thioester formation with E6AP HECT domain. ^{35}S-labeled E6AP HECT (43 kDa) was translated in a rabbit reticulocyte lysate cell-free translation system. Because the translation lysate supposedly contained ubiquitin (8 kDa), E1, and E2, the expressed E6AP HECT would be endogenously converted to the ubiquitin-adduct (E6AP HECT-Ub, 51 kDa). The translation mixture was treated with various concentrations of peptides (10^{-3}–10 μM) at room temperature for 30 min. The resulting mixtures were analyzed by SDS-PAGE without DTT. §When the Ub-thioester formation on E6AP was inhibited by CM_{11}-1 (as well as 10 μM LM_{11}-1), a slower migrating band than Ub-E6AP appeared on the gel. Although the product of this band has not yet been defined, this band disappeared upon addition of a free thiol reagent such as DTT (data not shown), suggesting a possibility of dimer formation of HECT domain via a disulfide bond. Alternatively, the free cysteine in HECT domain formed a disulfide bond with other proteins containing a free cysteine residue.

(B) Inhibition of E6-independent polyubiquitination on Prx1. $(His)_6$-Prx1 was incubated with 250 nM MEF-E6AP or inactive mutant MEF-E6AP^{C843A}, $(His)_6$-E1, $(His)_6$-UbcH7, ubiquitin and peptide at 37°C for 30 min. Reaction products were immunoprecipitated with anti-Prx1 pAb and visualized by antiubiquitin mAb immunoblotting. Asterisk denotes immunoglobulin heavy chain. ¶As a negative control, DMSO used as a cosolvent for CM_{11}-1 inhibition was added.

(C) Inhibition of E6-dependent polyubiquitination on p53. p53 was incubated with 170 nM MEF-E6AP, $(His)_6$-E1, $(His)_6$-UbcH7, ubiquitin, HPV16 E6, and peptide at 37°C for 30 min. Reaction products were immunoprecipitated with anti-p53 pAb and visualized by antiubiquitin mAb immunoblotting. See also Figure S4.

a Ub-thioester intermediate of the ^{35}S-Met-labeled HECT domain (Ub-HECT) was distinguished from the parental HECT domain by means of a SDS-PAGE mobility shift assay (Figure 4A, lane 1). When CM_{11}-1 was added to this translation assay system, the migration shift was suppressed at 1 μM or higher concentrations (lanes 5 and 6). As a negative control, LM_{11}-1 and CP_{11}-1 were also tested for the same inhibition assay, in which an approximately 50% inhibition was observed at 10 μM LM_{11}-1, whereas neither 1 μM LM_{11}-1 nor 10 μM CP_{11}-1 exhibited the inhibition. Although the observed potency by CM_{11}-1 seemed not as strong as expected from the SPR data, this could be attributed to that the RRL translation system might contain endogenous label-free E6AP (Huibregtse et al., 1991; Scheffner et al., 1993) that might interact with some fractions of CM_{11}-1, resulting in a reduction of the apparent inhibitory potency. Nevertheless, this result suggests that CM_{11}-1 is able to inhibit the charge of Ub onto the HECT domain of E6AP.

We then have further pursued testing inhibition of E6AP-catalyzed polyubiquitination on target proteins. Peroxiredoxin 1 (Prx1) is an endogenous substrate of E6AP in human cells, and its polyubiquitination occurs independently from the presence of E6 (Nasu et al., 2010). To monitor the inhibitory action of CM_{11}-1 against E6AP, we used an in vitro-reconstituted Prx1 polyubiquitination assay system, in which purified His-tagged Prx1 was incubated with E6AP tagged with MEF (Myc-TEV protease site-flag) and ubiquitin in the presence of purified His-tagged E1 and E2 (UbcH7). The resulting polyubiquitinated Prx1 (Prx1-Ub_n) and free Prx1 were immunoprecipitated by anti-Prx1 polyclonal antibodies and were immunoblotted by an anti-Ub monoclonal antibody to visualize in SDS-PAGE (Figure 4B, lanes 1–9). As negative controls, LM_{11}-1 and CP_{11}-1 were also included in this examination. Clearly, polyubiquitination of Prx1 was inhibited by CM_{11}-1 in a dose-dependent manner (lanes 5–9), where an approximately 1 μM of CM_{11}-1 nearly shut down the E6AP activity. On the other hand, neither LM_{11}-1 (lanes 10 and 11) nor CP_{11}-1 (data not shown) was able to inhibit polyubiquitination. We also tested Prx1-polyubiquitination inhibition by CM_{11}-1S_1, showing a weaker inhibitory activity than CM_{11}-1 (Figure S4); the result seemed consistent with the K_d values for both peptides observed in SPR experiments.

Finally, we examined the inhibitory activity of CM_{11}-1 against polyubiquitination on an E6-dependent substrate, p53, using a reconstituted p53 polyubiquitination assay system. Immunoprecipitation of poly- and nonubiquitinated p53 using anti-p53 pAb followed by immunobolotting using anti-Ub mAb enabled us to detect the polyUb-p53 on SDS-PAGE (Figure 4C). Again, 1 μM CM_{11}-1 was able to inhibit polyubiquitination of p53 in a dose-dependent manner (lanes 3–6), whereas the control peptide, LM_{11}-1, was not (lane 7). The result shows that CM_{11}-1 acts as an E6AP inhibitor that prevents polyubiquitination of Prx1 and p53 in E6-independent and E6-dependent manner, respectively. The trend of K_d values of CM_{11}-1 and its mutant peptides against E6AP HECT domain determined by the SPR experiments well reflected to their observed inhibitory behaviors against ubiquitination of target substrates (Table 1 and Figure 4). Because the present assay method allowed us to detect polyubiquitination instead of monoubiquitination of the substrate proteins catalyzed by an excess amount of E6AP (greater than

two orders of magnitude) over the inherent K_d value of CM_{11}-1, the observed inhibitory potency of CM_{11}-1 was only qualitatively assessed. Most importantly, CM_{11}-1 was capable of inhibiting Ub ligase activity of E6AP even though it was simply selected by binding to E6AP.

SIGNIFICANCE

Here, we have demonstrated RaPID selection of "natural product-like" peptides consisting of thioether-macrocyclic and N-methylated backbone. The selection against E6AP HECT domain has yielded such desired peptides with remarkable binding abilities, falling in a range of K_d values from a subnanomolar to a single-digit nanomolar. One of the representative peptides, CM_{11}-1, chosen for further studies has displayed inhibitory activity against E6AP-catalyzing polyubiquitination on the target proteins, Prx1 and p53. The present work provides the proof-of-technology of RaPID system that enables for the discovery of potent inhibitors against a previously nondruggable ubiquitin ligase, thus opening a wide range of possibilities in the discovery of inhibitors against other ubiquitin ligase families. Most importantly, the natural product-like macrocyclic *N*-methyl-peptides have larger interaction surfaces compared with small organic molecules, as well as elevated stability under physiological conditions compared with ordinary peptides; therefore, they would provide tremendous potentials for the development of drug leads that disrupt not only enzyme activities but also protein-protein interactions.

EXPERIMENTAL PROCEDURES

In Vitro Translation and Selection

Translation of the first round selection was performed using 100 pmol mRNA-puromycin (initial complexity is 6×10^{13}) and 150 μl of translation mixture in the presence of 3750 pmol of ClAc^{D}W-tRNA$^{fMet}_{CAU}$, ^{Me}G-tRNA$^{Asn\text{-}E2}_{GAU}$, ^{Me}A-tRNA$^{Asn\text{-}E2}_{GGC}$, ^{Me}S-tRNA$^{Asn\text{-}E2}_{GAG}$, and ^{Me}F-tRNA$^{Asn\text{-}E2}_{GAA}$ (25 μM each), at 37°C for 30 min. Subsequently, the translation mixture was incubated at room temperature for 12 min to conjugate the translated peptide with the corresponding mRNA-puromycin. This solution was incubation with 15 μl of 200 mM EDTA (pH 8.0) at 37°C for 30 min in order to dissociate ribosomes from mRNA-peptide complexes. For the first-round selection, 11 μl of E6AP HECT immobilized streptavidin magnetic beads (Dynabeads M-280, Invitrogen) was used at a concentration of 200 nM target protein, and mixed with the solution of mRNA-displayed *N*-methyl-peptides. The binding reaction was performed at 4°C for 30 min with rotation. After supernatant was removed, the bead was washed with 300 μl of cold wash buffer (100 mM Tris-HCl [pH 7.5], 300 mM NaCl, 0.05% [v/v] tween 20). To the bead was added 40 μl of RT reaction buffer (50 mM Tris-HCl [pH 8.3], 75 mM KCl, 3 mM $MgCl_2$, 10 μM DTT, 0.5 mM dNTPs, 2 μM CGS3an13.R39) containing 200 units of M-MLV reverse transcriptase (Promega) and 8 units of RNase inhibitor (Promega), and reverse transcribed at 42°C for 60 min with rotation. The selected cDNA was eluted with 360 μl of PCR buffer (10 mM Tris-HCl [pH 7.5], 50 mM KCl, 0.1% [v/v] Triton X-100, 2.5 mM $MgCl_2$, 0.25 mM dNTPs, 0.25 μM T7g10M.F48, 0.25 μM CGS3an13.R39) at 95°C for 5 min. After addition of *Taq* DNA polymerase to the eluate, the mixture was used for PCR amplification. The amplified DNA was purified by the extraction with phenol/chloroform and ethanol purification and was used for the next round of selection. Since the second round, 10 μl scale of transcription and 7.5 μl of ligation with puromycin linker were carried out. The resulting mRNA-puromycin of the second round was translated using 5 μl of the translation mixture in the presence of each 25 μM acyl-tRNAs at 37°C for 30 min, followed by incubation at room temperature for 12 min. After incubation with 1 μl of 100 mM EDTA (pH 8.0) at 37°C for 30 min, the reverse transcription of the mRNA-displayed peptides was performed by RT reaction buffer in the presence of M-MLV reverse transcriptase without RNase H activity (Promega), at 42°C for 60 min with rotation. After quenching the reaction with 1 μl of 100 mM EDTA (pH 8.0), the solution was neutralized with 1.1 μl of 0.2 M HCl. The complexes with cDNA- and mRNA-displayed peptides were subjected to 2.4 μl of the magnetic bead without target and were incubated at 4°C for 30 min for negative selection at once. Subsequently, the supernatant was mixed with 0.8 μl of the magnetic bead with E6AP HECT and was incubated with 4°C for 30 min for positive selection, followed by thrice washing with 10 μl of cold wash buffer. After addition of 100 μl of PCR buffer to the bead, the cDNA were eluted at 95°C for 5 min and amplified by *Taq* DNA polymerase. In the third round and all subsequent rounds, the all experiments were performed by a half of the reaction scale of the second round. Moreover, negative selection was performed at 4°C for 20 min at three times in the third and fourth round, and at nine times in the fifth and sixth round. On the other hand, positive selections after second round were performed by mixing with the complexes of cDNA and mRNA-displayed peptides and 200 nM E6AP HECT (not immobilized on streptavidin magnetic bead) at 37°C for 30 min, followed by pull down by streptavidin magnetic bead at 37°C for 5 min with rotation. After thrice washing with 5 μl of wash buffer at room temperature, the selected cDNA was eluted with 100 μl of PCR buffer at 95°C for 5 min. After addition of *Taq* DNA polymerase to the eluate, the mixture was used for PCR amplification. To monitor the convergence of the selection process, real-time PCR (RT-PCR) was used to quantify the amounts of input and output DNA in every round. For input cDNA, 0.25 μl aliquot of the RT mixture was diluted with 150 μl of a dilution solution (10 mM Tris-HCl [pH 8.0] and 300 mM NaCl), and 1 μl of the diluted cDNA was mixed with 19 μl of PCR buffer containing SYBR Green I (Molecular Probe) and *Taq* DNA polymerase. For output cDNA, 1 μl aliquots of the eluates from the beads of positive and negative selections were mixed with 10 μl of PCR buffer containing SYBR Green I and *Taq* DNA polymerase. The reverse transcribed $(NNU)_{10}$ mRNA mixture was serial-diluted and used for the templates as standards.

MALDI-TOF Analysis of Translated Clone Peptides

To identify the expressed cyclic *N*-methylated peptides, a 5 μl scale translation reaction was performed using FIT system with 40 nM of clone DNA, 25 μM each of ClAc^{D}W-tRNA$^{fMet}_{CAU}$, ^{Me}G-tRNA$^{Asn\text{-}E2}_{GAU}$, ^{Me}A-tRNA$^{Asn\text{-}E2}_{GGC}$, ^{Me}S-tRNA$^{Asn\text{-}E2}_{GAG}$, and ^{Me}F-tRNA$^{Asn\text{-}E2}_{GAA}$ at 37°C for 30 min. After quenching with 0.2% TFA, the crude peptide mixture was desalted with C-Tip (C18 desalting SPE, Nikkyo technos) and eluted with 80% acetonitrile and 0.5% acetic acid solution saturated with the matrix α-cyano-4-hydroxycinnamic acid (Bruker Daltonics). MALDI-TOF analysis was performed using an Autoflex TOF/TOF (Bruker Daltonics) and peptide calibration standard II (Bruker Daltonics) as external standards.

SPR Analysis of Peptides

The interaction between E6AP HECT and peptides was assessed using a BIACORE T100 instrument (GE Healthcare) equipped with research-grade streptavidin sensor chip at 25°C. Biotinylated E6AP HECT was immobilized to a surface density of approximate 1,500 response units (RU) using standard immobilization protocols (GE Healthcare). HBS-EP+ (10 mM HEPES [pH 7.4], 150 mM NaCl, 3 mM EDTA, and 0.05% [v/v] surfactant P20) containing 1.0% (v/v) DMSO was used as the running buffer for all experiments. Peptide binding was tested by injecting varying concentrations (0.3 nM to 1,000 nM) at a flow rate of 30 μl min^{-1} and measured by single cycle kinetics method. Raw data were analyzed by the BIACORE T100 evaluation software 2.01 and fitted to the standard 1:1 interaction model.

In Vitro Ubiquitin Transfer Assay by ^{35}S-Labeled E6AP HECT

E6AP HECT cDNA was subcloned into pTNT vector (Promega) at XhoI and SalI sites. ^{35}S-Methionine-labeled E6AP HECT was synthesized in vitro by TNT T7 coupled rabbit reticulocyte lysate system (Promega) at 30°C for 90 min, by following the standard procedure (Huibregtse et al., 1995). After translation, 0.5 μl of peptides in 10% (v/v) DMSO with 10× concentrations shown in Figure 4A were added to the translation reaction mixture (4.5 μL). The resulting mixture was incubated at room temperature at 30 min and

quenched with 2 × SDS-polyacrylamide gel laemli sample buffer (125 mM Tris-HCl [pH 6.8], SDS 4%, glycerol 20%, 0.002% bromophenol blue) in the absence of dithiothreitol. Samples were subjected to SDS-PAGE on a 10% polyacrylamide gel.

In Vitro Polyubiquitination Assay for Prx1 and p53

The plasmid pGEM p53 was used for in vitro translation (Werness et al., 1990). In vitro translation was performed using TNT T7 coupled rabbit reticulocyte lysate system. Recombinant baculovirus for HPV16 E6 was produced using the BaculoGold system (PharMingen) as described previously (Shirakura et al., 2007). Hi5 cells (Invitrogen) were infected with the recombinant baculovirus to produce HPV16 E6 protein. HPV16 E6 Protein was partially purified by anion-exchange chromatography as previously described (Huibregtse et al., 1993). In vitro polyubiquitination assays for Prx1 were performed essentially as described previously (Nasu et al., 2010). Hi5 cells were infected with recombinant baculoviruses AcMEF-E6AP and Ac MEF-E6AP^{C843A} to produce MEF-E6AP and MEF-E6AP^{C843A}, respectively (Shirakura et al., 2007). MEF-E6AP and MEF-E6AP^{C843A} were purified on anti-FLAG M2 agarose beads (Sigma) according to the manufacturer's instructions. Assays were done in 40 μl volumes containing 20 mM Tris (pH 7.6), 50 mM NaCl, 5 mM $MgCl_2$, 100 μM DTT, 5 mM ATP, 250 nM MEF-E6AP or inactive mutant MEF-E6AP^{C843A}, 62.5 nM $(His)_6$-E1, 1.1 μM $(His)_6$-UbcH7, 25 μM ubiquitin, 8 μM $(His)_6$-Prx1 and peptide, and incubation at 37°C for 30 min. Reactions were performed at 37°C for 30 min. The ubiquitination reaction was terminated by freezing the samples with liquid nitrogen. To dissociate proteins, 1% SDS was added to lysates, which were then heated at 90°C for 15 min. The samples were diluted 10-fold with a dissociation dilution buffer containing 1% NP-40, 0.5% deoxycholate, 120 mM NaCl, 50 mM HEPES, 1 mM EDTA, and complete protease inhibitor cocktail (Roche). Samples were immunoprecipitated with anti-Prx1 PAb and analysis by immunoblotting with antiubiquitin mouse monoclonal antibody (anti-Ubi-1, Millipore) to detect ubiquitinated Prx1. In vitro polyubiquitination assays for p53 were performed essentially as described previously (Nakagawa and Huibregtse, 2000). Assays were done in 75 μl volumes containing 25 mM Tris-HCl (pH 8.0), 125 mM NaCl, 2 mM $MgCl_2$, 50 μM DTT, 5 μM ubiquitin, 2 mM ATP, 170 nM MEF-E6AP, 33 nM $(His)_6$-E1, 0.6 μM $(His)_6$-UbcH7, 2 μl of partially purified HPV16 E6, and 5 μl of in vitro translated p53. Peptides inhibitors were added to the samples as indicated. The reaction mixtures were incubated at 37°C for 30 min. The ubiquitination reaction was terminated by freezing the samples with liquid nitrogen. To dissociate proteins, 1% SDS was added to lysates, which were then heated and diluted as described above. Samples were immunoprecipitated with anti-p53 rabbit polyclonal antibody (FL393, Santa Cruz), followed by immunoblotting with antiubiquitin mouse monoclonal antibody (anti-Ubi-1, Millipore) to detect ubiquitinated p53.

SUPPLEMENTAL INFORMATION

Supplemental Information includes four figures, one table, and supplemental Experimental Procedures and may be found with this article online at doi:10.1016/j.chembiol.2011.09.013.

ACKNOWLEDGMENTS

We thank Dr. Hiroshi Murakami for the discussion on conducting this work and Dr. Naoki Goshima for providing the cDNAs of E6AP and Smurf2. This work was supported by the Japan Society for the Promotion of Science (JSPS) Grants-in-Aid for the Specially Promoted Research (Grant 21000005), Research and Development Projects of the Industrial Science and Technology Program in the New Energy and Industrial Technology Development Organization (support to H.S.), Grants-in-Aid for JSPS Fellows (Grant 7734 to Y.Y.), JSPS Grants-in-Aid for Young Scientists (Grant B22710210 to T. Katoh and B22750145 to Y.G.), and Grants-in-Aid for Scientific Research from the Ministry of Health, Labour, and Welfare of Japan (to I.S. and H.S.).

Received: July 13, 2011
Revised: September 20, 2011
Accepted: September 20, 2011
Published: December 22, 2011

REFERENCES

Beaudenon, S., and Huibregtse, J.M. (2008). HPV E6, E6AP and cervical cancer. BMC Biochem. *9* (*Suppl 1*), S4.

Beaudenon, S., Dastur, A., and Huibregtse, J.M. (2005). Expression and assay of HECT domain ligases. Methods Enzymol. *398*, 112–125.

Biron, E., Chatterjee, J., Ovadia, O., Langenegger, D., Brueggen, J., Hoyer, D., Schmid, H.A., Jelinek, R., Gilon, C., Hoffman, A., and Kessler, H. (2008). Improving oral bioavailability of peptides by multiple N-methylation: somatostatin analogues. Angew. Chem. Int. Ed. Engl. *47*, 2595–2599.

Chatterjee, C., Paul, M., Xie, L., and van der Donk, W.A. (2005). Biosynthesis and mode of action of lantibiotics. Chem. Rev. *105*, 633–684.

Chatterjee, J., Gilon, C., Hoffman, A., and Kessler, H. (2008). N-methylation of peptides: a new perspective in medicinal chemistry. Acc. Chem. Res. *41*, 1331–1342.

Doedens, L., Opperer, F., Cai, M., Beck, J.G., Dedek, M., Palmer, E., Hruby, V.J., and Kessler, H. (2010). Multiple N-methylation of MT-II backbone amide bonds leads to melanocortin receptor subtype hMC1R selectivity: pharmacological and conformational studies. J. Am. Chem. Soc. *132*, 8115–8128.

Driggers, E.M., Hale, S.P., Lee, J., and Terrett, N.K. (2008). The exploration of macrocycles for drug discovery—an underexploited structural class. Nat. Rev. Drug Discov. *7*, 608–624.

Eldridge, A.G., and O'Brien, T. (2010). Therapeutic strategies within the ubiquitin proteasome system. Cell Death Differ. *17*, 4–13.

Eletr, Z.M., and Kuhlman, B. (2007). Sequence determinants of E2-E6AP binding affinity and specificity. J. Mol. Biol. *369*, 419–428.

Forster, A.C., Tan, Z., Nalam, M.N., Lin, H., Qu, H., Cornish, V.W., and Blacklow, S.C. (2003). Programming peptidomimetic syntheses by translating genetic codes designed *de novo*. Proc. Natl. Acad. Sci. USA *100*, 6353–6357.

Goto, Y., Ohta, A., Sako, Y., Yamagishi, Y., Murakami, H., and Suga, H. (2008). Reprogramming the translation initiation for the synthesis of physiologically stable cyclic peptides. ACS Chem. Biol. *3*, 120–129.

Goto, Y., Katoh, T., and Suga, H. (2011). Flexizymes for genetic code reprogramming. Nat. Protoc. *6*, 779–790.

Grünewald, J., and Marahiel, M.A. (2006). Chemoenzymatic and template-directed synthesis of bioactive macrocyclic peptides. Microbiol. Mol. Biol. Rev. *70*, 121–146.

Hershko, A., and Ciechanover, A. (1998). The ubiquitin system. Annu. Rev. Biochem. *67*, 425–479.

Hoeller, D., and Dikic, I. (2009). Targeting the ubiquitin system in cancer therapy. Nature *458*, 438–444.

Hoeller, D., Hecker, C.M., and Dikic, I. (2006). Ubiquitin and ubiquitin-like proteins in cancer pathogenesis. Nat. Rev. Cancer *6*, 776–788.

Huang, L., Kinnucan, E., Wang, G., Beaudenon, S., Howley, P.M., Huibregtse, J.M., and Pavletich, N.P. (1999). Structure of an E6AP-UbcH7 complex: insights into ubiquitination by the E2-E3 enzyme cascade. Science *286*, 1321–1326.

Huibregtse, J.M., Scheffner, M., and Howley, P.M. (1991). A cellular protein mediates association of p53 with the E6 oncoprotein of human papillomavirus types 16 or 18. EMBO J. *10*, 4129–4135.

Huibregtse, J.M., Scheffner, M., and Howley, P.M. (1993). Localization of the E6-AP regions that direct human papillomavirus E6 binding, association with p53, and ubiquitination of associated proteins. Mol. Cell. Biol. *13*, 4918–4927.

Huibregtse, J.M., Scheffner, M., Beaudenon, S., and Howley, P.M. (1995). A family of proteins structurally and functionally related to the E6-AP ubiquitin-protein ligase. Proc. Natl. Acad. Sci. USA *92*, 2563–2567.

Josephson, K., Hartman, M.C., and Szostak, J.W. (2005). Ribosomal synthesis of unnatural peptides. J. Am. Chem. Soc. *127*, 11727–11735.

Kawakami, T., Murakami, H., and Suga, H. (2008). Messenger RNA-programmed incorporation of multiple *N*-methyl-amino acids into linear and cyclic peptides. Chem. Biol. *15*, 32–42.

Kohli, R.M., Walsh, C.T., and Burkart, M.D. (2002). Biomimetic synthesis and optimization of cyclic peptide antibiotics. Nature *418*, 658–661.

Kumar, S., Talis, A.L., and Howley, P.M. (1999). Identification of HHR23A as a substrate for E6-associated protein-mediated ubiquitination. J. Biol. Chem. *274*, 18785–18792.

Kung, H.F., Redfield, B., Treadwell, B.V., Eskin, B., Spears, C., and Weissbach, H. (1977). DNA-directed in vitro synthesis of beta-galactosidase: studies with purified factors. J. Biol. Chem. *252*, 6889–6894.

Layfield, R., Lowe, J., and Bedford, L. (2005). The ubiquitin-proteasome system and neurodegenerative disorders. Essays Biochem. *41*, 157–171.

Li, P., and Roller, P.P. (2002). Cyclization strategies in peptide derived drug design. Curr. Top. Med. Chem. *2*, 325–341.

Liu, Y., Cherry, J.J., Dineen, J.V., Androphy, E.J., and Baleja, J.D. (2009). Determinants of stability for the E6 protein of papillomavirus type 16. J. Mol. Biol. *386*, 1123–1137.

Louria-Hayon, I., Alsheich-Bartok, O., Levav-Cohen, Y., Silberman, I., Berger, M., Grossman, T., Matentzoglu, K., Jiang, Y.H., Muller, S., Scheffner, M., et al. (2009). E6AP promotes the degradation of the PML tumor suppressor. Cell Death Differ. *16*, 1156–1166.

McIntosh, J.A., Donia, M.S., and Schmidt, E.W. (2009). Ribosomal peptide natural products: bridging the ribosomal and nonribosomal worlds. Nat. Prod. Rep. *26*, 537–559.

Murakami, H., Ohta, A., Ashigai, H., and Suga, H. (2006). A highly flexible tRNA acylation method for non-natural polypeptide synthesis. Nat. Methods *3*, 357–359.

Nakagawa, S., and Huibregtse, J.M. (2000). Human scribble (Vartul) is targeted for ubiquitin-mediated degradation by the high-risk papillomavirus E6 proteins and the E6AP ubiquitin-protein ligase. Mol. Cell. Biol. *20*, 8244–8253.

Nalepa, G., Rolfe, M., and Harper, J.W. (2006). Drug discovery in the ubiquitin-proteasome system. Nat. Rev. Drug Discov. *5*, 596–613.

Nasu, J., Murakami, K., Miyagawa, S., Yamashita, R., Ichimura, T., Wakita, T., Hotta, H., Miyamura, T., Suzuki, T., Satoh, T., and Shoji, I. (2010). E6AP ubiquitin ligase mediates ubiquitin-dependent degradation of peroxiredoxin 1. J. Cell. Biochem. *111*, 676–685.

Nemoto, N., Miyamoto-Sato, E., Husimi, Y., and Yanagawa, H. (1997). In vitro virus: bonding of mRNA bearing puromycin at the 3′-terminal end to the C-terminal end of its encoded protein on the ribosome *in vitro*. FEBS Lett. *414*, 405–408.

Nestor, J.J., Jr. (2009). The medicinal chemistry of peptides. Curr. Med. Chem. *16*, 4399–4418.

Ogunjimi, A.A., Briant, D.J., Pece-Barbara, N., Le Roy, C., Di Guglielmo, G.M., Kavsak, P., Rasmussen, R.K., Seet, B.T., Sicheri, F., and Wrana, J.L. (2005). Regulation of Smurf2 ubiquitin ligase activity by anchoring the E2 to the HECT domain. Mol. Cell *19*, 297–308.

Ohta, A., Murakami, H., Higashimura, E., and Suga, H. (2007). Synthesis of polyester by means of genetic code reprogramming. Chem. Biol. *14*, 1315–1322.

Ohta, A., Yamagishi, Y., and Suga, H. (2008). Synthesis of biopolymers using genetic code reprogramming. Curr. Opin. Chem. Biol. *12*, 159–167.

Ohuchi, M., Murakami, H., and Suga, H. (2007). The flexizyme system: a highly flexible tRNA aminoacylation tool for the translation apparatus. Curr. Opin. Chem. Biol. *11*, 537–542.

Oman, T.J., and van der Donk, W.A. (2010). Follow the leader: the use of leader peptides to guide natural product biosynthesis. Nat. Chem. Biol. *6*, 9–18.

Pickart, C.M. (2001). Mechanisms underlying ubiquitination. Annu. Rev. Biochem. *70*, 503–533.

Roberts, R.W., and Szostak, J.W. (1997). RNA-peptide fusions for the *in vitro* selection of peptides and proteins. Proc. Natl. Acad. Sci. USA *94*, 12297–12302.

Rubinsztein, D.C. (2006). The roles of intracellular protein-degradation pathways in neurodegeneration. Nature *443*, 780–786.

Sagan, S., Karoyan, P., Lequin, O., Chassaing, G., and Lavielle, S. (2004). N- and Calpha-methylation in biologically active peptides: synthesis, structural and functional aspects. Curr. Med. Chem. *11*, 2799–2822.

Scheffner, M., Werness, B.A., Huibregtse, J.M., Levine, A.J., and Howley, P.M. (1990). The E6 oncoprotein encoded by human papillomavirus types 16 and 18 promotes the degradation of p53. Cell *63*, 1129–1136.

Scheffner, M., Huibregtse, J.M., Vierstra, R.D., and Howley, P.M. (1993). The HPV-16 E6 and E6-AP complex functions as a ubiquitin-protein ligase in the ubiquitination of p53. Cell *75*, 495–505.

Scheffner, M., Nuber, U., and Huibregtse, J.M. (1995). Protein ubiquitination involving an E1-E2-E3 enzyme ubiquitin thioester cascade. Nature *373*, 81–83.

Shimizu, Y., Inoue, A., Tomari, Y., Suzuki, T., Yokogawa, T., Nishikawa, K., and Ueda, T. (2001). Cell-free translation reconstituted with purified components. Nat. Biotechnol. *19*, 751–755.

Shirakura, M., Murakami, K., Ichimura, T., Suzuki, R., Shimoji, T., Fukuda, K., Abe, K., Sato, S., Fukasawa, M., Yamakawa, Y., et al. (2007). E6AP ubiquitin ligase mediates ubiquitylation and degradation of hepatitis C virus core protein. J. Virol. *81*, 1174–1185.

Werness, B.A., Levine, A.J., and Howley, P.M. (1990). Association of human papillomavirus types 16 and 18 E6 proteins with p53. Science *248*, 76–79.

Zhou, P., Lugovskoy, A.A., and Wagner, G.A. (2001). A solubility-enhancement tag (SET) for NMR studies of poorly behaving proteins. J. Biomol. NMR *20*, 11–14.

frontiers in
MICROBIOLOGY

MINI REVIEW ARTICLE
published: 10 January 2012
doi: 10.3389/fmicb.2011.00278

Molecular mechanism of hepatitis C virus-induced glucose metabolic disorders

Ikuo Shoji*, Lin Deng and Hak Hotta

Division of Microbiology, Center for Infectious Diseases, Kobe University Graduate School of Medicine, Kobe, Japan

Edited by:
Yasuko Yokota, National Institute of Infectious Diseases, Japan

Reviewed by:
Koji Ishii, National Institute of Infectious Diseases, Japan
Kohji Moriishi, University of Yamanashi, Japan

****Correspondence:***
Ikuo Shoji, Division of Microbiology, Center for Infectious Diseases, Kobe University Graduate School of Medicine, 7-5-1 Kusunoki-cho, Chuo-ku, Kobe, Hyogo 650-0017, Japan.
e-mail: ishoji@med.kobe-u.ac.jp

Hepatitis C virus (HCV) infection causes not only intrahepatic diseases but also extrahepatic manifestations, including metabolic disorders. Chronic HCV infection is often associated with type 2 diabetes. However, the precise mechanism underlying this association is still unclear. Glucose is transported into hepatocytes via glucose transporter 2 (GLUT2). Hepatocytes play a crucial role in maintaining plasma glucose homeostasis via the gluconeogenic and glycolytic pathways. We have been investigating the molecular mechanism of HCV-related type 2 diabetes using HCV RNA replicon cells and HCV J6/JFH1 system. We found that HCV replication down-regulates cell surface expression of GLUT2 at the transcriptional level. We also found that HCV infection promotes hepatic gluconeogenesis in HCV J6/JFH1-infected Huh-7.5 cells. HCV infection transcriptionally up-regulated the genes for phosphoenolpyruvate carboxykinase (PEPCK) and glucose 6-phosphatase (G6Pase), the rate-limiting enzymes for hepatic gluconeogenesis. Gene expression of PEPCK and G6Pase was regulated by the transcription factor forkhead box O1 (FoxO1) in HCV-infected cells. Phosphorylation of FoxO1 at Ser319 was markedly diminished in HCV-infected cells, resulting in increased nuclear accumulation of FoxO1. HCV NS5A protein was directly linked with the FoxO1-dependent increased gluconeogenesis. This paper will discuss the current model of HCV-induced glucose metabolic disorders.

Keywords: HCV, diabetes, gluconeogenesis, GLUT2, FoxO1, JNK, NS5A

INTRODUCTION

Hepatitis C virus (HCV) is a positive-sense, single stranded RNA virus that belongs to the genus *Hepacivirus* of the family *Flaviviridae*. The approximately 9.6-kb HCV genome encodes a unique open reading frame that is translated into a polyprotein of about 3,000 amino acids, which is cleaved by cellular signalases and viral proteases to generate at least 10 viral proteins, such as core, envelope 1 (E1) and E2, p7, NS2, NS3, NS4A, NS4B, NS5A, and NS5B (Choo et al., 1991; Lemon et al., 2007).

Hepatitis C virus is the main cause of chronic hepatitis, liver cirrhosis, and hepatocellular carcinoma. More than 170 million people worldwide are chronically infected with HCV (Poynard et al., 2003). Persistent HCV infection causes not only liver diseases but also extrahepatic manifestations. It is well established that HCV perturbs the glucose metabolism, leading to insulin resistance and type 2 diabetes in predisposed individuals. Several epidemiological, clinical, and experimental data suggested that HCV infection serves as an additional risk factor for the development of diabetes (Mason et al., 1999; Negro and Alaei, 2009; Negro, 2011). HCV-related glucose metabolic changes and insulin resistance and diabetes have significant clinical consequences, such as accelerated fibrogenesis, increased incidence of hepatocellular carcinoma, and reduced virological response to interferon (IFN)-α-based therapy (Negro, 2011). Therefore, it is very important to clarify the molecular mechanism of HCV-related diabetes. However, the precise mechanisms are poorly understood.

Experimental data suggest a direct interference of HCV with the insulin signaling pathway. Transgenic mice expressing HCV core gene exhibit insulin resistance (Shintani et al., 2004; Koike, 2007). In this transgenic mice model, both tyrosine phosphorylation of the insulin receptor substrate (IRS)-1 and IRS-2 are decreased. These decreases are recovered when the proteasome activator PA28γ is deleted, suggesting that the HCV core protein suppresses insulin signaling through a PA28γ-dependent pathway (Miyamoto et al., 2007). Several other reports also showed a link of the HCV core protein with insulin resistance (Kawaguchi et al., 2004; Pazienza et al., 2007).

Hepatocytes play a crucial role in maintaining plasma glucose homeostasis by adjusting the balance between hepatic glucose production and utilization via the gluconeogenic and glycolytic pathways, respectively. Gluconeogenesis is mainly regulated at the transcriptional level of the glucose 6-phosphatase (G6Pase) and phosphoenolpyruvate carboxykinase (PEPCK) genes, whereas glycolysis is mainly regulated by glucokinase (GK). Gluconeogenesis and glycolysis are coordinated so that one pathway is highly active within a cell while the other is relatively inactive. It is well known that increased hepatic glucose production via gluconeogenesis is a major feature of type 2 diabetes (Clore et al., 2000).

To identify a novel mechanism of HCV-related diabetes, we have been investigating the effects of HCV on glucose production in hepatocytes using HCV RNA replicon cells (Lohmann et al., 1999) and HCV J6/JFH1 cell culture system (Lindenbach et al., 2005; Wakita et al., 2005; Bungyoku et al., 2009). We previously reported that HCV replication suppresses cellular glucose uptake through down-regulation of cell surface expression of glucose transporter 2 (GLUT2; Kasai et al., 2009). Furthermore, we

recently reported that HCV promotes hepatic gluconeogenesis via an NS5A-mediated, forkhead box O1 (FoxO1)-dependent pathway, resulting in increased cellular glucose production in hepatocytes (Deng et al., 2011). This paper discusses our current model for HCV-induced glucose metabolic disorders.

HCV REPLICATION DOWN-REGULATES CELL SURFACE EXPRESSION OF GLUT2

The uptake of glucose into cells is conducted by the facilitative glucose carrier, glucose transporters (GLUTs). GLUTs are integral membrane proteins that contain 12 membrane-spanning helices. To date, a total of 14 isoforms have been identified in the GLUT family (Wu and Freeze, 2002; Macheda et al., 2005; Godoy et al., 2006). Glucose is transported into hepatocytes by GLUT2. We previously reported that HCV J6/JFH1 infection suppresses hepatocytic glucose uptake through down-regulation of surface expression of GLUT2 in human hepatoma cell line, Huh-7.5 cells (Kasai et al., 2009). We also demonstrated that GLUT2 expression in hepatocytes of the liver tissues from HCV-infected patients was significantly lower than in those from patients without HCV infection. Our data suggest that HCV infection down-regulates GLUT2 expression at transcriptional level. We are currently analyzing transcriptional control of human GLUT2 promoter in HCV replicon cells as well as in HCV J6/JFH1-infected cells.

HCV INFECTION PROMOTES HEPATIC GLUCONEOGENESIS

Then we analyzed hepatic glucose production and expression of transcription factors using HCV replicon cells and HCVcc system in order to clarify a role of HCV infection in glucose metabolic changes. Hepatic glucose production is usually regulated by gluconeogenesis and glycolysis. Therefore, we examined whether HCV infection induces gluconeogenesis or glycolysis. We found that the PEPCK and G6Pase genes were transcriptionally up-regulated in J6/JFH1-infected cells (**Figure 1**). On the other hand, the GK gene was transcriptionally down-regulated in HCV-infected cells. We obtained similar data in HCV replicon cells (both in subgenomic replicon cells and full-genomic replicon cells). When HCV replication was suppressed by IFN treatment, the up-regulation of PEPCK and G6Pase gene expression as well as the down-regulation of GK gene expression were canceled. From these results, HCV infection selectively up-regulates PEPCK and G6Pase genes, whereas HCV infection down-regulates GK gene (Deng et al., 2011).

Both HCV replicon cells and HCV-infected cells produced greater amounts of glucose than the control cells. IFN treatment canceled the enhanced glucose production in HCV replicon cells as well as in HCV-infected cells. G6P is an important precursor molecule that is converted to glucose in the gluconeogenesis pathway (**Figure 1**). Our metabolite analysis showed that a significantly higher level of G6P was accumulated in HCV-infected cells than in the control cells, suggesting that HCV indeed promotes hepatic gluconeogenesis to cause hyperglycemia. There is a trend toward an increase in gluconeogenesis in HCV-infected cells (**Figure 1**).

HCV SUPPRESSES FoxO1 PHOSPHORYLATION AT Ser319, LEADING TO THE NUCLEAR ACCUMULATION OF FoxO1

It has been reported that G6Pase, PEPCK, and GK are regulated by certain transcription factors, including FoxO1 (Hirota et al., 2008), hepatic nuclear factor 4α (HNF-4α; Hirota et al.,

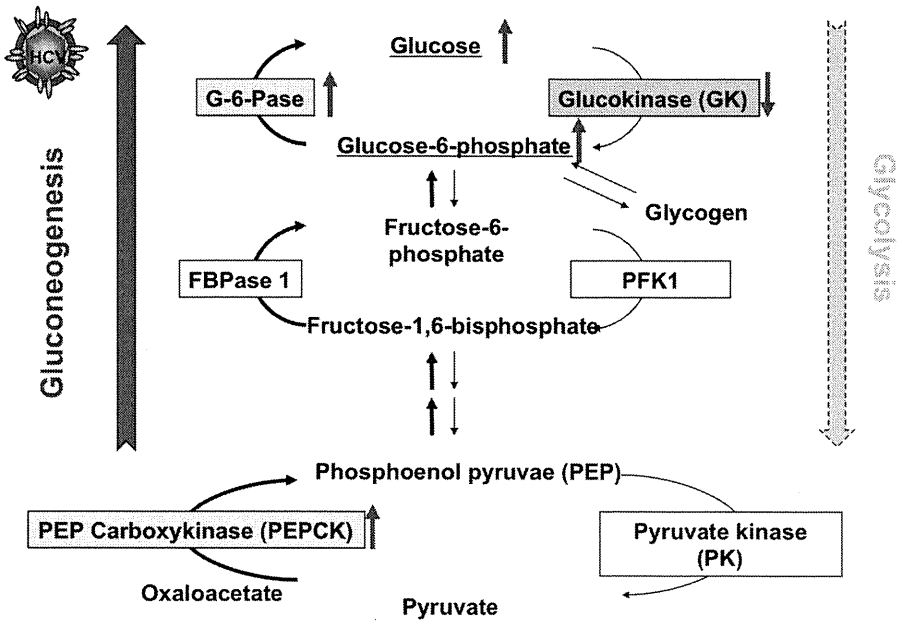

FIGURE 1 | Regulation of Gluconeogenesis and Glycolysis in the HCV-infected cells. HCV infection promotes gluconeogenesis via transcriptional up-regulation of the genes for PEPCK and G6Pase, the rate-limiting enzymes for hepatic gluconeogenesis, and transcriptional down-regulation of the gene for GK, the rate-limiting enzyme for hepatic glycolysis.

2008), Krüppel-like factor 15 (KLF15; Takashima et al., 2010), and cyclic AMP (cAMP) response element binding protein (CREB; Rozance et al., 2008). While we were analyzing these factors in both HCV replicon cells and HCV J6/JFH1-infected cells, we found the involvement of the FoxO1 in the transcriptional activation of G6Pase and PEPCK (Deng et al., 2011). It is known that the FoxO1 enhances gluconeogenesis through the transcriptional activation of various genes, including G6Pase and PEPCK (Gross et al., 2008). The function of FoxO1 is regulated by post-translational modifications, including phosphorylation, ubiquitylation, and acetylation (Tzivion et al., 2011). The phosphorylated form of FoxO1 is exported from the nucleus to the cytosol, resulting in loss of its transcriptional activity (**Figure 2**). Phosphorylation status of FoxO1 at Ser319 is critical for FoxO1 nuclear exclusion (Zhao et al., 2004). Although the total amounts of FoxO1 protein were unchanged, FoxO1 phosphorylation at Ser319 was markedly suppressed in HCV-infected cells compared to that in the mock-infected cells. It is known that the FoxO1 is phosphorylated by the protein kinase Akt and is exported from the nucleus to the cytosol, resulting in loss of its transcriptional activity (Tzivion et al., 2011). The majority of FoxO1 was accumulated in the nuclear fraction in HCV-infected cells, whereas in control cells FoxO1 was distributed in both the nuclear and cytoplasmic fractions. Akt phosphorylation was enhanced in HCV-infected cells, although the protein levels of total Akt protein were comparable, which is consistent with the report by Burdette et al. (2010). Our findings suggest an interesting scenario in which the HCV-mediated suppression in FoxO1 phosphorylation is caused by an unknown mechanism independent of Akt activity.

HCV-INDUCED JNK ACTIVATION IS INVOLVED IN THE SUPPRESSION OF FoxO1 PHOSPHORYLATION

It is known that the stress-sensitive serine/threonine kinase JNK regulates FoxO at multiple levels (van der Horst and Burgering, 2007; Karpac and Jasper, 2009). We demonstrated that HCV infection induces phosphorylation and activation of JNK in a time-dependent manner, which is similar to that observed for the suppression of FoxO1 phosphorylation. As a result, c-Jun, a key substrate for JNK, got phosphorylated and activated in HCV-infected cells. The JNK inhibitor SP600125 clearly prevented the phosphorylation of c-Jun, and concomitantly recovered the suppression of FoxO1 phosphorylation in HCV-infected cells, suggesting that HCV activates the JNK/c-Jun signaling pathway, resulting in the nuclear accumulation of FoxO1 by reducing its phosphorylation status. The detailed mechanisms of HCV-induced suppression of FoxO1 phosphorylation via the JNK/c-Jun signaling pathway remain to be explored. There are at least two possibilities. The JNK/c-Jun signaling pathway (1) suppresses a protein kinase, or (2) activates a protein phosphatase to reduce phosphorylation of FoxO1.

HCV-INDUCED MITOCHONDRIAL REACTIVE OXYGEN SPECIES PRODUCTION IS INVOLVED IN INCREASED GLUCOSE PRODUCTION THROUGH JNK ACTIVATION

Hepatitis C virus infection increases mitochondrial reactive oxygen species (ROS) production (Deng et al., 2008). *N*-acetyl cysteine (NAC; a general antioxidant) clearly prevented the phosphorylation of JNK, and concomitantly canceled the suppression of FoxO1 phosphorylation in HCV-infected cells, suggesting that

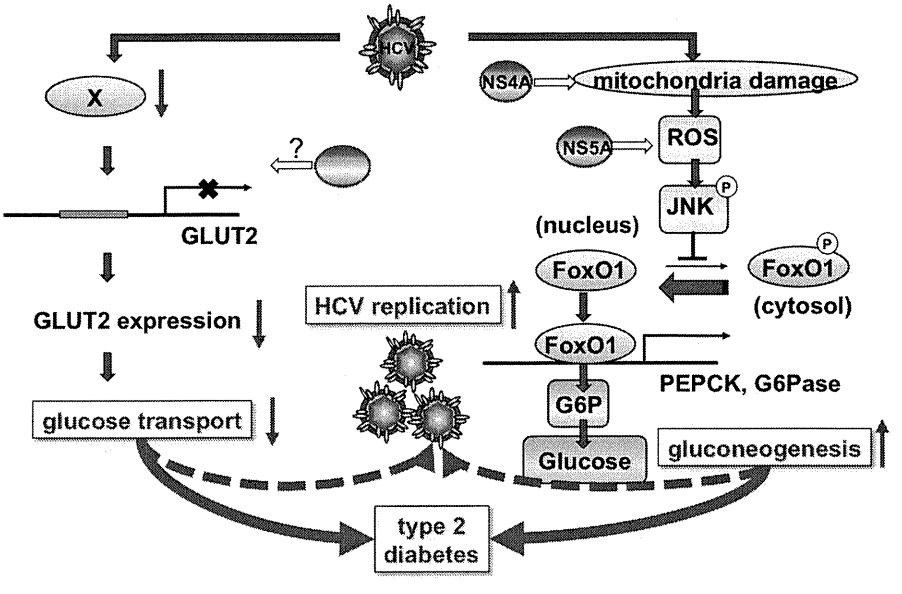

FIGURE 2 | A proposed mechanism of HCV-induced glucose metabolic disorders. HCV infection down-regulates cell surface expression of GLUT2 in hepatocytes at the transcriptional level. HCV down-regulates a transcription factor involved in GLUT2 gene expression through an unknown mechanism. HCV infection induces mitochondria damage and ROS production, leading to JNK activation. HCV NS4A protein is involved in mitochondrial damage. HCV NS5A protein is involved in ROS production. HCV-induced ROS production causes JNK activation, resulting in the decreased phosphorylation and nuclear accumulation of FoxO1. Nuclear accumulation of FoxO1 up-regulates gene expression of PEPCK and G6Pase, leading eventually to increased glucose production by gluconeogenesis. High glucose levels in the hepatocytes may confer an advantage in efficient replication of HCV.

HCV-induced ROS production is involved in the JNK activation. There was no significant difference in HCV RNA replication or infectious virus release between SP600125- or NAC-treated HCV-infected cells and non-treated HCV-infected cells. These results suggest that ROS-mediated JNK activation plays a key role in the suppression of FoxO1 phosphorylation, nuclear accumulation of FoxO1, and enhancement of glucose production in HCV-infected cells (Deng et al., 2011).

HCV NS5A IS INVOLVED IN THE ENHANCEMENT OF GLUCOSE PRODUCTION

Then we sought to determine which HCV protein(s) is involved in the enhancement of glucose production. Transient expression of NS5A protein in Huh-7.5 cells significantly promoted the gene expression levels of G6Pase and PEPCK determined by real time quantitative RT-PCR. Promoter assay revealed that the level of PEPCK promoter activity was significantly higher in NS5A-expressing cells than in the control cells. Our results suggest that NS5A activate both the PEPCK promoter and the G6Pase promoter, leading to an increase in glucose production (Deng et al., 2011). The study by Banerjee et al. (2010) suggests that the HCV core protein modulates FoxO1 and FoxA2 activation and affects insulin-induced metabolic gene regulation in human hepatocytes. Our results, however, suggest that the HCV core protein is not significantly involved in the increased gluconeogenesis (Deng et al., 2011). The difference between these two studies needs to be explored.

There were previous reports suggesting that ROS production is induced in NS5A-expressing cells (Dionisio et al., 2009) or in hepatocytes of NS5A transgenic mice (Wang et al., 2009). We therefore sought to determine whether NS5A contributes to increased hepatic gluconeogenesis through the induction of ROS production. NS5A-expressing cells displayed a much stronger signal of ROS than in control cells. NS5A-expressing cells promoted phosphorylation level at Ser63 of c-Jun and suppressed FoxO1 phosphorylation at Ser319, suggesting that NS5A mediates JNK/c-Jun activation and FoxO1 phosphorylation suppression. These results suggest that NS5A play a role in the HCV-induced enhancement of hepatic gluconeogenesis through JNK/c-Jun activation and FoxO1 phosphorylation suppression.

CONCLUSION AND FUTURE PERSPECTIVES

Taken together, we propose a model of HCV-induced glucose metabolic disorders as shown in **Figure 2**. HCV infection down-regulates cell surface expression of GLUT2 in hepatocytes at the transcriptional level. HCV down-regulates a transcription factor involved in GLUT2 gene expression through an unknown mechanism. As GLUT2 is a facilitative GLUT, it ensures large bidirectional fluxes of glucose in and out the cell due to its low affinity and high capacity (Leturque et al., 2009). Down-regulated cell surface expression of GLUT2 results in disruption of bidirectional transport of glucose in hepatocytes. Even in the fasting state, down-regulation of GLUT2 may result in low glucose uptake of hepatocytes, causing hyperglycemia. In the fed state, glucose secretion from hepatocytes may be suppressed due to low level cell surface expression of GLUT2, as GLUT2 is a bidirectional transporter.

Hepatitis C virus infection induces mitochondria damage and ROS production, leading to JNK activation. HCV NS4A protein is involved in mitochondrial damage (Nomura-Takigawa et al., 2006). HCV NS5A protein is involved in ROS production (Dionisio et al., 2009; Wang et al., 2009; Deng et al., 2011). HCV-induced ROS production causes JNK activation, which results in the decreased phosphorylation and nuclear accumulation of FoxO1 by an unidentified mechanism. Nuclear accumulation of FoxO1 up-regulates gene expression of PEPCK and G6Pase, leading eventually to increased glucose production by gluconeogenesis (Deng et al., 2011).

These two pathways, HCV-induced down-regulation of GLUT2 expression and up-regulation of gluconeogenesis, may contribute to development of type 2 diabetes in HCV-infected patients at least to some extent. HCV-induced down-regulation of GLUT2 expression and up-regulation of gluconeogenesis may result in high concentration of glucose in HCV-infected hepatocytes. As suggested in a recent study, low glucose concentration in the hepatocytes inhibits HCV replication (Nakashima et al., 2011). Therefore, high glucose levels in the hepatocytes may confer an advantage in efficient replication of HCV.

Our understanding of HCV-induced glucose metabolic disorders will require much more work to fully unfold this pathway. Further investigation including the mechanism of HCV-induced GLUT2 downregualtion, JNK-mediated decreased phosphorylation of FoxO1, and the possible effect(s) of the dysregulation of hepatic gluconeogenesis on the HCV life cycle and host cells are currently under way.

ACKNOWLEDGMENTS

The authors are grateful to all of their co-workers who contributed to the studies cited here. This work was supported in part by grants-in-aid for Research on Hepatitis from the Ministry of Health, Labor and Welfare, Japan, and the Japan Initiative for Global Research Network on Infectious Diseases (J-GRID) program of Ministry of Education, Culture, Sports, Science and Technology, Japan. This study was also carried out as part of the Global Center of Excellence program of Kobe University Graduate School of Medicine, and the Science and Technology Research Partnership for Sustainable Development (SATREPS) program of Japan Science and Technology Agency (JST) and Japan International Cooperation Agency (JICA).

REFERENCES

Banerjee, A., Meyer, K., Mazumdar, B., Ray, R. B., and Ray, R. (2010). Hepatitis C virus differentially modulates activation of forkhead transcription factors and insulin-induced metabolic gene expression. *J. Virol.* 84, 5936–5946.

Bungyoku, Y., Shoji, I., Makine, T., Adachi, T., Hayashida, K., Nagano-Fujii, M., Ide, Y. H., Deng, L., and Hotta, H. (2009). Efficient production of infectious hepatitis C virus with adaptive mutations in cultured hepatoma cells. *J. Gen. Virol.* 90, 1681–1691.

Burdette, D., Olivarez, M., and Waris, G. (2010). Activation of transcription factor Nrf2 by hepatitis C virus induces the cell-survival pathway. *J. Gen. Virol.* 91, 681–690.

Choo, Q. L., Richman, K. H., Han, J. H., Berger, K., Lee, C., Dong, C., Gallegos, C., Coit, D., Medina-Selby,

R., Barr, P. J., Weiner, A. J., Bradley, D. W., Kuo, G., and Houghton, M. (1991). Genetic organization and diversity of the hepatitis C virus. *Proc. Natl. Acad. Sci. U.S.A.* 88, 2451–2455.

Clore, J. N., Stillman, J., and Sugerman, H. (2000). Glucose-6-phosphatase flux in vitro is increased in type 2 diabetes. *Diabetes* 49, 969–974.

Deng, L., Adachi, T., Kitayama, K., Bungyoku, Y., Kitazawa, S., Ishido, S., Shoji, I., and Hotta, H. (2008). Hepatitis C virus infection induces apoptosis through a Bax-triggered, mitochondrion-mediated, caspase 3-dependent pathway. *J. Virol.* 82, 10375–10385.

Deng, L., Shoji, I., Ogawa, W., Kaneda, S., Soga, T., Jiang, D. P., Ide, Y. H., and Hotta, H. (2011). Hepatitis C virus infection promotes hepatic gluconeogenesis through an NS5A-mediated, FoxO1-dependent pathway. *J. Virol.* 85, 8556–8568.

Dionisio, N., Garcia-Mediavilla, M. V., Sanchez-Campos, S., Majano, P. L., Benedicto, I., Rosado, J. A., Salido, G. M., and Gonzalez-Gallego, J. (2009). Hepatitis C virus NS5A and core proteins induce oxidative stress-mediated calcium signalling alterations in hepatocytes. *J. Hepatol.* 50, 872–882.

Godoy, A., Ulloa, V., Rodriguez, F., Reinicke, K., Yanez, A. J., Garcia Mde, L., Medina, R. A., Carrasco, M., Barberis, S., Castro, T., Martinez, F., Koch, X., Vera, J. C., Poblete, M. T., Figueroa, C. D., Peruzzo, B., Perez, F., and Nualart, F. (2006). Differential subcellular distribution of glucose transporters GLUT1-6 and GLUT9 in human cancer: ultrastructural localization of GLUT1 and GLUT5 in breast tumor tissues. *J. Cell. Physiol.* 207, 614–627.

Gross, D. N., van den Heuvel, A. P., and Birnbaum, M. J. (2008). The role of FoxO in the regulation of metabolism. *Oncogene* 27, 2320–2336.

Hirota, K., Sakamaki, J., Ishida, J., Shimamoto, Y., Nishihara, S., Kodama, N., Ohta, K., Yamamoto, M., Tanimoto, K., and Fukamizu, A. (2008). A combination of HNF-4 and Foxo1 is required for reciprocal transcriptional regulation of glucokinase and glucose-6-phosphatase genes in response to fasting and feeding. *J. Biol. Chem.* 283, 32432–32441.

Karpac, J., and Jasper, H. (2009). Insulin and JNK: optimizing metabolic homeostasis and lifespan. *Trends Endocrinol. Metab.* 20, 100–106.

Kasai, D., Adachi, T., Deng, L., Nagano-Fujii, M., Sada, K., Ikeda, M., Kato, N., Ide, Y. H., Shoji, I., and Hotta, H. (2009). HCV replication suppresses cellular glucose uptake through down-regulation of cell surface expression of glucose transporters. *J. Hepatol.* 50, 883–894.

Kawaguchi, T., Yoshida, T., Harada, M., Hisamoto, T., Nagao, Y., Ide, T., Taniguchi, E., Kumemura, H., Hanada, S., Maeyama, M., Baba, S., Koga, H., Kumashiro, R., Ueno, T., Ogata, H., Yoshimura, A., and Sata, M. (2004). Hepatitis C virus down-regulates insulin receptor substrates 1 and 2 through up-regulation of suppressor of cytokine signaling 3. *Am. J. Pathol.* 165, 1499–1508.

Koike, K. (2007). Hepatitis C virus contributes to hepatocarcinogenesis by modulating metabolic and intracellular signaling pathways. *J. Gastroenterol. Hepatol.* 22(Suppl. 1), S108–S111.

Lemon, S. M., Walker, C., Alter, M. J., and Yi, M. (2007). "Hepatitis C virus," in *Fields' Virology*, 5th Edn, eds B. N. Fields, D. M. Knipe, and P. M. Howley (Philadelphia, PA: Wolters Kluwer Health/Lippincott Williams and Wilkins), 1291–1304.

Leturque, A., Brot-Laroche, E., and Le Gall, M. (2009). GLUT2 mutations, translocation, and receptor function in diet sugar managing. *Am. J. Physiol. Endocrinol. Metab.* 296, E985–E992.

Lindenbach, B. D., Evans, M. J., Syder, A. J., Wolk, B., Tellinghuisen, T. L., Liu, C. C., Maruyama, T., Hynes, R. O., Burton, D. R., McKeating, J. A., and Rice, C. M. (2005). Complete replication of hepatitis C virus in cell culture. *Science* 309, 623–626.

Lohmann, V., Korner, F., Koch, J., Herian, U., Theilmann, L., and Bartenschlager, R. (1999). Replication of subgenomic hepatitis C virus RNAs in a hepatoma cell line. *Science* 285, 110–113.

Macheda, M. L., Rogers, S., and Best, J. D. (2005). Molecular and cellular regulation of glucose transporter (GLUT) proteins in cancer. *J. Cell. Physiol.* 202, 654–662.

Mason, A. L., Lau, J. Y., Hoang, N., Qian, K., Alexander, G. J., Xu, L., Guo, L., Jacob, S., Regenstein, F. G., Zimmerman, R., Everhart, J. E., Wasserfall, C., Maclaren, N. K., and Perrillo, R. P. (1999). Association of diabetes mellitus and chronic hepatitis C virus infection. *Hepatology* 29, 328–333.

Miyamoto, H., Moriishi, K., Moriya, K., Murata, S., Tanaka, K., Suzuki, T., Miyamura, T., Koike, K., and Matsuura, Y. (2007). Involvement of the PA28gamma-dependent pathway in insulin resistance induced by hepatitis C virus core protein. *J. Virol.* 81, 1727–1735.

Nakashima, K., Takeuchi, K., Chihara, K., Hotta, H., and Sada, K. (2011). Inhibition of hepatitis C virus replication through adenosine monophosphate-activated protein kinase-dependent and -independent pathways. *Microbiol. Immunol.* 55, 774–782.

Negro, F. (2011). Mechanisms of hepatitis C virus-related insulin resistance. *Clin. Res. Hepatol. Gastroenterol.* 35, 358–363.

Negro, F., and Alaei, M. (2009). Hepatitis C virus and type 2 diabetes. *World J. Gastroenterol.* 15, 1537–1547.

Nomura-Takigawa, Y., Nagano-Fujii, M., Deng, L., Kitazawa, S., Ishido, S., Sada, K., and Hotta, H. (2006). Non-structural protein 4A of Hepatitis C virus accumulates on mitochondria and renders the cells prone to undergoing mitochondria-mediated apoptosis. *J. Gen. Virol.* 87, 1935–1945.

Pazienza, V., Clement, S., Pugnale, P., Conzelman, S., Foti, M., Mangia, A., and Negro, F. (2007). The hepatitis C virus core protein of genotypes 3a and 1b downregulates insulin receptor substrate 1 through genotype-specific mechanisms. *Hepatology* 45, 1164–1171.

Poynard, T., Yuen, M. F., Ratziu, V., and Lai, C. L. (2003). Viral hepatitis C. *Lancet* 362, 2095–2100.

Rozance, P. J., Limesand, S. W., Barry, J. S., Brown, L. D., Thorn, S. R., LoTurco, D., Regnault, T. R., Friedman, J. E. and Hay, W. W. Jr. (2008). Chronic late-gestation hypoglycemia upregulates hepatic PEPCK associated with increased PGC1alpha mRNA and phosphorylated CREB in fetal sheep. *Am. J. Physiol. Endocrinol. Metab.* 294, E365–E370.

Shintani, Y., Fujie, H., Miyoshi, H., Tsutsumi, T., Tsukamoto, K., Kimura, S., Moriya, K., and Koike, K. (2004). Hepatitis C virus infection and diabetes: direct involvement of the virus in the development of insulin resistance. *Gastroenterology* 126, 840–848.

Takashima, M., Ogawa, W., Hayashi, K., Inoue, H., Kinoshita, S., Okamoto, Y., Sakaue, H., Wataoka, Y., Emi, A., Senga, Y., Matsuki, Y., Watanabe, E., Hiramatsu, R., and Kasuga, M. (2010). Role of KLF15 in regulation of hepatic gluconeogenesis and metformin action. *Diabetes* 59, 1608–1615.

Tzivion, G., Dobson, M., and Ramakrishnan, G. (2011). FoxO transcription factors; Regulation by AKT and 14-3-3 proteins. *Biochim. Biophys. Acta* 1813, 1938–1945.

van der Horst, A., and Burgering, B. M. (2007). Stressing the role of FoxO proteins in lifespan and disease. *Nat. Rev. Mol. Cell Biol.* 8, 440–450.

Wakita, T., Pietschmann, T., Kato, T., Date, T., Miyamoto, M., Zhao, Z., Murthy, K., Habermann, A., Krausslich, H. G., Mizokami, M., Bartenschlager, R., and Liang, T. J. (2005). Production of infectious hepatitis C virus in tissue culture from a cloned viral genome. *Nat. Med.* 11, 791–796.

Wang, A. G., Lee, D. S., Moon, H. B., Kim, J. M., Cho, K. H., Choi, S. H., Ha, H. L., Han, Y. H., Kim, D. G., Hwang, S. B., and Yu, D. Y. (2009). Non-structural 5A protein of hepatitis C virus induces a range of liver pathology in transgenic mice. *J. Pathol.* 219, 253–262.

Wu, X., and Freeze, H. H. (2002). GLUT14, a duplicon of GLUT3, is specifically expressed in testis as alternative splice forms. *Genomics* 80, 553–557.

Zhao, X., Gan, L., Pan, H., Kan, D., Majeski, M., Adam, S. A., and Unterman, T. G. (2004). Multiple elements regulate nuclear/cytoplasmic shuttling of FOXO1: characterization of phosphorylation- and 14-3-3-dependent and -independent mechanisms. *Biochem. J.* 378, 839–849.

Conflict of Interest Statement: The authors declare that the research was conducted in the absence of any commercial or financial relationships that could be construed as a potential conflict of interest.

Received: 01 December 2011; accepted: 25 December 2011; published online: 10 January 2012.

Citation: Shoji I, Deng L and Hotta H (2012) Molecular mechanism of hepatitis C virus-induced glucose metabolic disorders. Front. Microbio. 2:278. doi: 10.3389/fmicb.2011.00278

This article was submitted to Frontiers in Virology, a specialty of Frontiers in Microbiology.

ELSEVIER

Institut Pasteur

Microbes and Infection 14 (2012) 69–78

www.elsevier.com/locate/micinf

Original article

Generation of a recombinant reporter hepatitis C virus useful for the analyses of virus entry, intra-cellular replication and virion production

Kazuya Kamada [a], Ikuo Shoji [a], Lin Deng [a], Chie Aoki [a,b], Suratno Lulut Ratnoglik [a,b], Takaji Wakita [c], Hak Hotta [a,b,*]

[a] *Division of Microbiology, Kobe University, Graduate School of Medicine, 7-5-1 Kusunoki-cho, Cyuo-ku, Kobe, Hyogo 650-0017, Japan*
[b] *JST/JICA SATREPS, Japan*
[c] *Department of Virology II, National Institute of Infectious Diseases, Shinjuku-ku, Tokyo 162-8640, Japan*

Received 21 February 2011; accepted 18 August 2011
Available online 31 August 2011

Abstract

The lack of a culture system that efficiently produces progeny virus has hampered hepatitis C virus (HCV) research. Recently, the discovery of a novel HCV isolate JFH1 and its chimeric derivative J6/JFH1 has led to the development of an efficient virus productive culture system. To construct an easy monitoring system for the viral life cycle of HCV, we generated bicistronic luciferase reporter virus genomes based on the JFH1 and J6/JFH1 isolates, respectively. Transfection of the J6/JFH1-based reporter genome to Huh7.5 cells produced significantly greater levels of progeny virus than transfection of the JFH1 genome. Furthermore, the expression of dominant-negative Vps4, a key molecule of the endosomal sorting complex required for transport machinery, inhibited the virus production of JFH1, but not that of J6/JFH1. These results may account for the different abilities to produce progeny virus between JFH1 and J6/JFH1. Using the J6/JFH1/Luc system, we showed that the two polyanions heparin and polyvinyl sulfate decreased the infectivity of J6/JFH1/Luc virus in a dose-dependent manner. We also analyzed the function of microRNA on HCV replication and found that miR-34b could affect the replication of HCV. The reporter virus generated in this study will be useful for investigating the nature of the HCV life cycle and for identification of HCV inhibitors.

Keywords: HCV; Reporter virus; Virus production; ESCRT; microRNA

1. Introduction

Hepatitis C virus (HCV) is an enveloped virus and has a positive-stranded RNA genome of about 9.6 kb [1,2]. HCV persistently infects hepatocytes, and the persistent infection can lead to liver cirrhosis and hepatocellular carcinoma. Considering that approximately 170 million people are infected with HCV worldwide [3], HCV is a major public health problem throughout the world. A combination therapy of pegylated interferon-α and ribavirin has been established as the standard of care for treating HCV infection [3,4]. Nonetheless, approximately 50% of individuals with chronic HCV infection are still unable to resolve infection [4,5]. For this reason, more effective therapies are greatly needed against the disease caused by HCV infection [6].

The HCV genome encodes a 3000 amino acid polyprotein which is cleaved by host and viral proteases to yield the mature structural proteins, composed of core and glycoprotein E1 and E2, and the non-structural proteins p7, NS2, NS3, NS4A, NS4B, NS5A, and NS5B [1–3]. Translation of the HCV open reading frames is mediated via the 5′ untranslated region and a part of the core coding region carrying the internal ribosome entry site (IRES) [1,7].

In 1999, Bartenschlager and his colleagues produced the HCV replicon system, a tissue culture system that recapitulated the RNA replication of HCV in a human hepatoma cell line [8]. In the initial subgenomic replicon system, genes

* Corresponding author. Division of Microbiology, Kobe University, Graduate School of Medicine, 7-5-1 Kusunoki-cho, Cyuo-ku, Kobe, Hyogo 650-0017, Japan. Tel.: +81 78 382 5500; fax: +81 78 382 5519.
E-mail address: hotta@kobe-u.ac.jp (H. Hotta).

1286-4579/$ - see front matter © 2011 Institut Pasteur. Published by Elsevier Masson SAS. All rights reserved.
doi:10.1016/j.micinf.2011.08.009

unessential for RNA replication that contained the core, E1, E2, p7 and NS2 of the HCV genome were replaced with a genetic cassette carrying an antibiotics resistance gene and IRES from encephalomyocarditis virus (EMCV). The development of a subgenomic replicon system became a driving force for the studies on the mechanism of HCV replication, and these studies revealed numerous biological features of HCV replication. However, the resulting systems were unable to produce progeny virus. Therefore, the nature of the HCV, i.e., the virus production and virus entry, remained unclear for a long while.

Wakita and his colleagues isolated a full-length HCV genome from the sera of a patient with fulminant hepatitis [9]. The HCV strain, designated JFH1, belongs to genotype 2a. The transfection of the Huh7 hepatoma cell line with the JFH1 genome yields a progeny virus called HCVcc that is infectious both *in vivo* and *in vitro*. The HCVcc system allowed us to perform virological studies to investigate the nature of HCV [9,10]. However, the analyses using HCVcc have not been suitable for carrying out high-throughput screening due to the labor-intensive quantitative reverse transcription-PCR methods used in screening and the difficulties presented by the low signal-to-noise ratios.

In this study, to develop a robust tool for use in the screening of HCV replication, we have constructed a genome-length luciferase reporter HCV derived from the JFH1 and J6/JFH1 strains, and used it to analyze the intra-cellular RNA replication and extra-cellular progeny virus production. We demonstrated here that our recombinant reporter HCV system was useful for studying viral genome replication, virus entry, and virion production of HCV.

2. Materials and methods

2.1. Plasmids

The plasmid pFGR-JFH1/Luc, which encodes bicistronic constructs of HCV IRES-driven firefly luciferase reporter genes and the EMCV IRES-driven full-genomic JFH1 genome, was constructed by insertion of the JFH1 full genome of pJFH1 [9] into pSGR-JFH1 [11]. The plasmid pFL-J6/JFH1, which contains a chimeric full-genome composed of the 5′NCR to NS2 region derived from J6 and NS3 to the 3′NCR region from JFH1 [10], was kindly supplied by C.M. Rice of the Center for the Study of Hepatitis C, Rockefeller University. To yield the bicistronic luciferase reporter construct composed of full-length J6/JFH1, the JFH1 full genome of pFGR-JFH1/Luc was replaced with the J6/JFH1 full genome of pFL-J6/JFH1 by digestion with BstZ17I, and the resultant plasmid was designated as pFGR-J6/JFH1/Luc. As a negative control for the HCV replication, a non-synonymous mutation at NS5B (GDD to GND), which disrupts NS5B polymerase activity, was introduced into the pFGR-J6/JFH1/Luc NS5B region by site-directed mutagenesis, and the resultant plasmid was designated pFGR-J6/JFH1/Luc (GND).

2.2. Cell culture and indirect immunofluorescence

All experiments described in this study were performed by using Huh7.5 human hepatoma cells, a highly HCV-susceptible subclone of Huh7 cells. The cells were cultured in Dulbecco's minimum essential medium (DMEM) supplemented with 10% heat-inactivated fetal bovine serum, 2 mM glutamine, and 0.01% streptomycin, and were subcultured twice weekly. Huh7.5 cells electroporated with JFH1/Luc or J6/JFH1/Luc RNA were subjected to indirect immunofluorescence analysis as previously reported [12]. The primary antibody used was derived from an HCV-infected patient's serum. The secondary antibody used was fluorescein isothiocyanate (FITC)-conjugated goat anti-human IgG (MBL, Nagoya, Japan).

2.3. In vitro transcription and electroporation

Plasmid DNA was linearized with XbaI, extracted with phenol and chloroform, precipitated with ethanol, and dissolved in RNase-free water. The purified DNA was used for *in vitro* RNA transcription using a T7 Megascript kit (Ambion, Austin, TX) following the manufacturer's protocols. The concentration was determined by measurement of the optical density at 260 nm, and the RNA integrity was checked by agarose gel electrophoresis. The *in vitro*-transcribed RNA (10 μg) was transfected into Huh7.5 cells by means of electroporation (975 μF, 270 V) using a Gene Pulser (Bio-Rad, Hercules, CA). The cells were then cultured in complete medium. The culture fluid of transfected cells was harvested and cleared by passing through 0.45-μm-pore-size filters and stored at −80 °C until use.

2.4. Luciferase assay

The *firefly* luciferase activity was measured by a luciferase assay system (Promega, Madison, WS). The cells were harvested, washed twice with dication-free phosphate buffered saline (PBS), and lysed in a passive lysis buffer supplied by the manufacturer. A 20-μl sample of the lysate was subjected to a luciferase assay. The luminescence was measured at 10 s after an initial 2 s delay according to the manufacturer's instructions, using a Lumat LB9501 luminometer (Berthold, Freiburg, Germany). The assays were performed in duplicate at least three times, and the mean and standard error were computed.

2.5. Vectors of ESCRT family proteins and DNA transfection

The cDNA of the endosomal sorting complex required for transport (ESCRT) family proteins was amplified from Huh7.5 cells by RT-PCR and cloned into pcDNA3.1-FLAG [13], an expression vector containing a CMV promoter and FLAG tag sequence in pcDNA3.1 (Invitrogen, Carlsbad, CA). For the expression of each ESCRT family protein, Huh7.5 cells were transfected with each ESCRT expression vector by using TransIT LT1 transfection reagents (Takara, Kyoto, Japan). The expression levels of the three ESCRT family proteins in

transfected Huh7.5 cells were monitored by immunoblotting using the anti-FLAG antibody (Sigma–Aldrich, St. Louis, MO).

2.6. Quantification of HCV core protein

HCV core protein in the cells or cell-culture supernatants was quantified by using a highly sensitive enzyme immunoassay (Ortho HCV antigen ELISA kit; Ortho Clinical Diagnostics). To determine the intra-cellular amounts of core, cell lysates were prepared as described by Schaller et al. [14].

2.7. Blocking of virus attachment and entry with anti-CD81 antibody

Blocking of virus attachment and entry with anti-CD81 antibody was performed essentially as described previously [9]. Huh7.5 cells (6×10^4 cells/well of a 24-well plate) were pre-treated with anti-CD81 antibody (clone JS-81; BD Biosciences) or an isotype-matched control antibody (purified mouse IgG1, isotype control; BD Biosciences) as indicated for 1 h. Cells were then infected with the reporter viruses for 6 h. The viruses were removed, and then the culture medium was replaced with complete DMEM. On day 2 post-infection, the cells were lysed with a passive lysis buffer as mentioned above. The efficiency of infection was monitored by measuring the luciferase activity of the cell lysate.

2.8. Transfection of microRNA inhibitor

Huh7.5 cells were electroporated with luciferase reporter HCV RNA as mentioned above, and then the cells were seeded in a well of a 24-well plate. To analyze the effect of inhibition of microRNA (miR), both a specific miRNA inhibitor (Anti-miR™ miRNA) and a non-targeting negative control (Anti-miR™miRNA Inhibitors—Negative Control) were purchased from Ambion, Inc. 50 pmol of a specific miRNA inhibitor or negative control were transfected into luciferase reporter RNA-electroporated Huh7.5 cells by using a siPORT™ NeoFX™ Transfection Agent (Ambion) according to the manufacturer's instructions. At 48 h post-transfection, the cells were harvested, and viral replication was determined by luciferase assay of the cell lysate.

2.9. Polyions

The polyanions heparin (mol. wt. 3000), dextran sulfate (mol. wt. 50,000) and polyvinyl sulfate (mol. wt. 150,000), and the polycations polybrene (mol. wt. 3000), DEAE-dextran (mol. wt. 100,000), and poly-L-lysine (mol. wt. 500,000) (all purchased from Sigma) were dissolved in PBS.

3. Results

3.1. Construction and characterization of luciferase reporter HCV

To construct a reporter HCV that can permit easy monitoring of both virus production and intra-cellular viral growth kinetics, we constructed the bicistronic HCV constructs by inserting a luciferase reporter gene into the 5′ end of the coding sequence of the JFH1 or J6/JFH1 full-genome plasmids clone as shown in Fig. 1A. In the transcript derived from bicistronic reporter HCV clone, the HCV and EMCV IRESs are responsible for the translation of the luciferase protein and all HCV proteins, respectively. A reporter construct with NS5B GDD to GND mutation, which disrupts viral polymerase function, was also constructed by site-directed mutagenesis, and served as a negative control for viral genome replication. To examine the replication level of reporter HCVs, we prepared the RNAs from each construct by *in vitro* transcription, and then transfected them into Huh7.5 cells by an electroporation technique. The viral replication was quantified up to 10 days post-transfection by using an HCV core-specific ELISA and luciferase reporter assay. As shown in Fig. 1B, the transfection of RNAs of both the JFH1/Luc and J6/JFH1/Luc reporter clones induced intra-cellular HCV core protein expression, which peaked on day 2 post-transfection. Both JFH1/Luc and J6/JFH1/Luc showed similar kinetics, and the high level core protein expression continued until day 10 post-transfection. As expected, the GND mutant exhibited 100-fold lower intra-cellular core protein expression on day 2 post-transfection. The level of core expression by the GND mutant continued to decline thereafter, and fell below the detection limit on day 10 post-transfection. As shown in Fig. 1C, both JFH1/Luc and J6/JFH1/Luc induced similar levels of luciferase activity in Huh7.5 cells at 4 h after electroporation. This result indicated that both RNAs were electroporated with similar efficiency because RNA replication had not started at that time and all the luciferase was translated from the input RNA. At 4 days post-electroporation, the luciferase activities of both JFH1/Luc and J6/JFH1/Luc were 10-fold greater than those measured at 4 h after electroporation. Subsequently, JFH1/Luc and J6/JFH1/Luc showed almost the same kinetics of luciferase activity until 10 days post-transfection. At 3 days post-electroporation, both JFH1/Luc and J6/JFH1/Luc electroporated cells were stained with HCV-positive patient sera, and the rate of intra-cellular replication was then visualized using immunofluorescent microscopy as previously reported [12]. As a result, the HCV-positive rates were 17% and 19% for JFH1/Luc and J6/JFH1/Luc, respectively (Fig. 1D). These results indicated that the luciferase activity of reporter HCV-transfected cells reflected the intra-cellular viral replication, and also suggested that both JFH1 and J6/JFH1 had similar intra-cellular replication ability in Huh7.5 cells.

3.2. Production of cell-free infectious progeny virions in luciferase reporter HCV RNA-transfected cells

Next, we assessed the potential of the reporter HCV to produce infectious progeny virions. Huh7.5 cells were electroporated with the reporter RNAs, and the culture supernatant was collected at various time points. To analyze the release of progeny virions from the reporter RNA-electroporated cells, the amounts of core protein in culture supernatants were

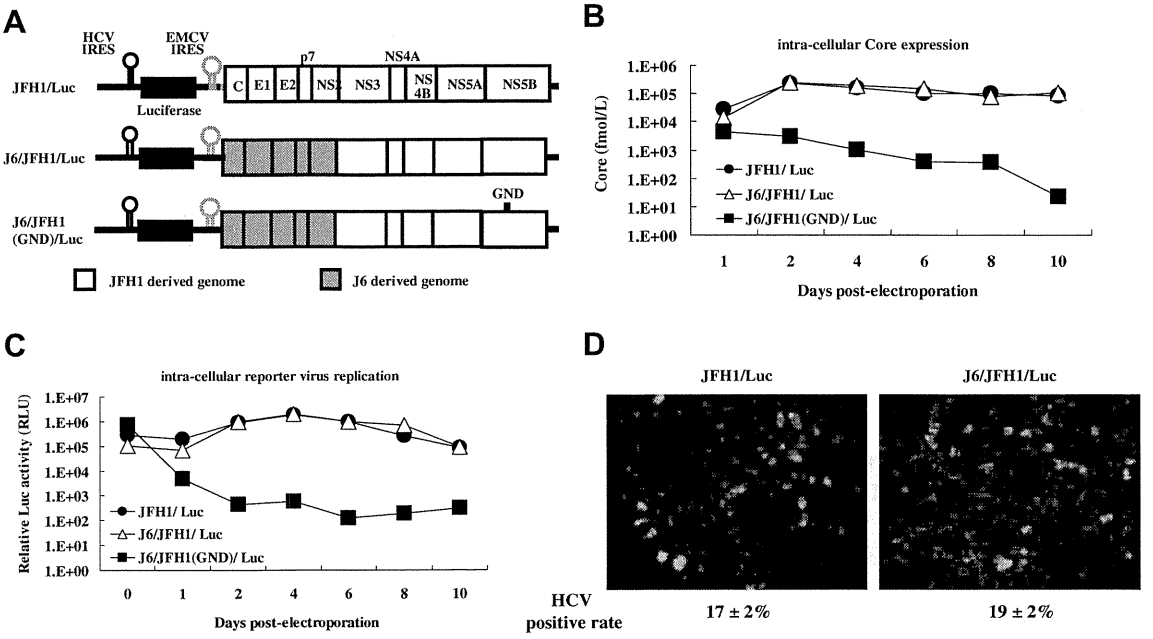

Fig. 1. Schematics of luciferase reporter HCV in this study. (A) Organization of luciferase reporter HCV. The luciferase gene is depicted as a black box. The JFH1-derived open reading frame and J6-derived open reading frame are depicted as a gray box and white box, respectively. As a negative control, a GND mutation was introduced to NS5B RdRp. (B, C) Virus replication kinetics in Huh7.5 cells of luciferase reporter HCV. The cells were electroporated with luciferase reporter RNA as described in Materials and methods, and the cells were assayed for core protein ELISA (B) and luciferase activity (C) at intervals as indicated. The assays were repeated at least three times, and the mean values are presented. Huh7.5 cells electroporated with JFH1/Luc or J6/JFH1/Luc RNA were subjected to indirect immunofluorescence analysis at 3 days post-electroporation (D). Cells were incubated with an HCV-infected patient's serum followed by FITC-labeled goat anti-human IgG (green). In parallel, the cells were stained with Hoechst 33342 to visualize the nuclei (blue). The HCV-positive rate was calculated by counting the number of HCV-positive cells among the total cells, and the data represent the means and SE of three independent experiments.

analyzed by ELISA. As shown in Fig. 2A, electroporation of both reporter viral RNAs with Huh7.5 cells released the HCV core protein into the culture supernatants. The levels of core protein released from both reporter HCV RNAs peaked at 6 days post-electroporation. The amount of core protein of the J6/JFH1/Luc supernatants was 2–4 fold greater than that of JFH1/Luc among all the time points tested. In parallel, to analyze the infectivity of progeny virions produced from reporter RNA-electroporated cells, these supernatants were used as inocula for naïve Huh7.5 cells. The cells inoculated with these supernatants were harvested at 48 h post-inoculation, and the luciferase activity of the cell lysate was analyzed (Fig. 2B). These supernatants infected naïve Huh7.5 cells, and transduced luciferase activity in the cells. The infectious virus of both reporter HCVs was initially detected on day 2 and peaked on day 4 post-electroporation. However, the infectivity was decreased after day 6 post-electroporation. Furthermore, the infectivity of J6/JFH1/Luc supernatants was significantly higher than that of JFH1/Luc (approximately 10-fold). To compare the luciferase activity and the virus titer, we

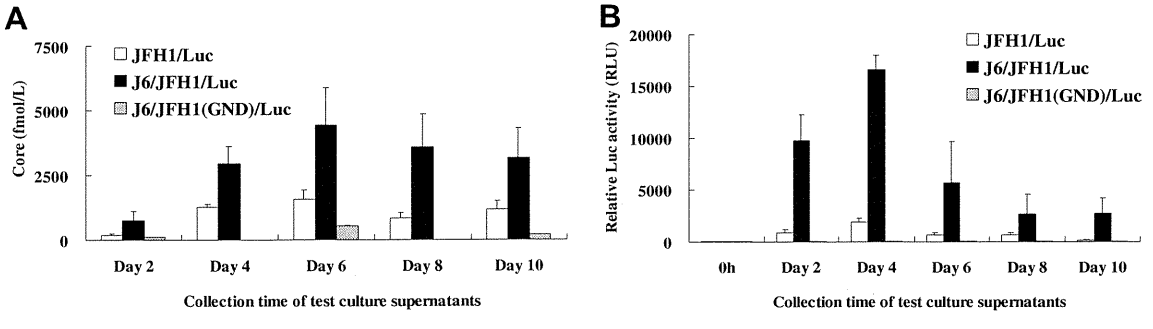

Fig. 2. Progeny virus production from luciferase reporter RNA-transfected Huh7.5 cells. The cells were electroporated with luciferase reporter RNA as described in Materials and methods, and culture supernatants of the cells were collected at the indicated time points. The amount of progeny virus in the supernatant was measured by the HCV core protein ELISA. (A) In parallel, the supernatants were added to naïve Huh7.5 cells. At 48 h post-addition, the cells were lysed, and assayed for luciferase activity to assess the infectivity of progeny virus from reporter HCV RNA. (B) The assays were repeated at least three times, and the mean values are presented.

performed standard virion titration by immunofluorescent antibody staining. The result showed that the virus titer of J6/JFH/Luc supernatant, collected at day 4 post-RNA transfection, was 5×10^3 fluorescent-focus forming units (ffu) per ml. In contrast, the titer of JFH/Luc supernatant was below the detection limit ($<1 \times 10^2$ ffu/ml). Interestingly, the peaks of the core release and the infectivity were slightly different, i.e., the peak of the core release of J6/JFH1 was on day 6, and that of the infectivity was on day 4 post-electroporation. Collectively, these data revealed that J6/JFH1 had a greater ability to release progeny virions than JFH1, though the levels of intracellular replication were comparable between J6/JFH1/and JFH1.

3.3. Characterization of cell-free infectious progeny virions in luciferase reporter HCV RNA-transfected cells

Next, we examined whether the J6/JFH1/Luc-derived supernatants had the features of a virus and thus could be used as a surrogate for HCV. The supernatants collected from each culture of reporter RNA-electroporated cells were irradiated with ultra-violet (UV) for 5 min, and the supernatants were then inoculated into naïve Huh7.5 cells. As shown in Fig. 3A, the infectivity of the reporter virus was completely abrogated by UV-irradiation. The results indicated that the luciferase activity transduced by the supernatants was derived from the genome of the reporter virus, not from incorporation of the luciferase protein into the virion. The entry of the HCV virion was mediated by binding between the cellular surface protein CD81 and the HCV envelope protein E2 [15]. Therefore, the naïve Huh7.5 cells were pre-treated with a recombinant monoclonal antibody against CD81. After 1 h pre-treatment, the J6/JFH1/Luc supernatant was inoculated into the cells, and the luciferase activity of cells was analyzed at 48 h post-inoculation (Fig. 3B). Normal mouse IgG showed no effect on the infectivity of the J6/JFH/Luc supernatant. In contrast, the infectivity of the J6/JFH/Luc supernatant was decreased by pre-treatment with anti-CD81 antibody in a dose-dependent manner. The results suggested that the supernatant from luciferase reporter J6/JFH1/Luc-transfected cells contained a virus with characteristics similar to HCV, and that this reporter virus could be utilized to investigate all the steps of virus replication, including the intra-cellular viral replication, the virus production and the virus entry as a surrogate model of HCV.

3.4. Analysis of a potential role for ESCRT family proteins in HCV virus production

Prior to the recent establishment of the JFH1-based cell-culture system, there was no system for producing the HCV virus, and thus many aspects of the virus production of HCV still remain poorly understood. Generally, the production of the enveloped virus requires a multi-step process that includes the proper transport of viral proteins and organization of viral proteins on the cellular membrane, and these steps are coordinated by a variety of cellular factors [16,17]. From numerous intensive studies, it has been revealed that the process of budding of many enveloped viruses utilizes the ESCRT machinery, which is responsible for the formation of luminal vesicles of endosomal multivesicular bodies (MVB) [16,18–20]. The ESCRT machinery consists of a number of cellular proteins that make up three functional sub-complexes – ESCRT-I, ESCRT-II and ESCRT-III – and other related factors; i.e., Vps4 and AIP/Alix are also participated in the function of ESCRT machinery [20]. A series of analyses about ESCRT networks has revealed the consensus amino acid motifs of viral proteins; the P(T/S)AP motif was observed to interact with Tsg101, and the YPxL motif was seen in the case of AIP/Ailx [19]. We searched for these motifs in the J6 and JFH1 genomes, and found one AIP/Alix interacting the YPxL motif in the NS5B region (aa. 2604 to 2607; YPDL). Therefore, the relation between ESCRT and HCV was examined by analyzing the virus production using a luciferase reporter HCV system. First, we constructed the expression plasmids of the ESCRT-I protein Tsg101, and the ESCRT-associated proteins Nedd4L and AIP/Alix. The ESCRT expression plasmids were transfected into the J6/JFH1/Luc or JFH1/Luc RNA-transfected Huh7.5 cells. After 48 h of transfection, the culture supernatants were collected and inoculated into the culture of the naïve Huh7.5 cells. The effects of over-expression of ESCRT proteins on intra-cellular virus

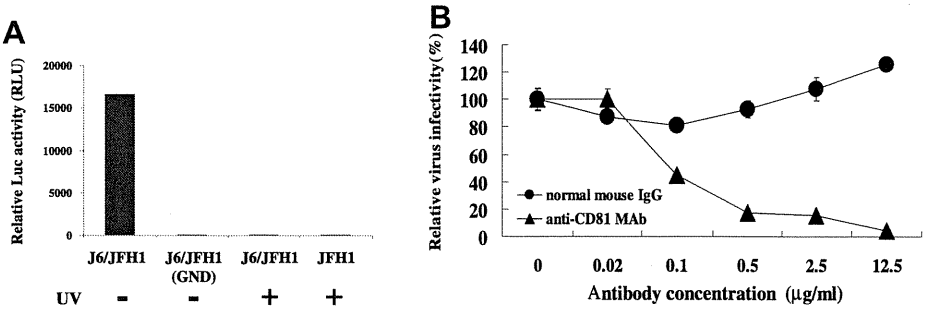

Fig. 3. Anti-CD81 antibody blocks luciferase reporter HCV infection. The reporter viruses containing supernatants were prepared as described in Materials and methods. (A) The JFH1/Luc and J6/JFH1/Luc supernatants were irradiated with UV at 5 min, and then added to naïve Huh7.5 cells. The infectivity was analyzed by luciferase assay. (B) Huh7.5 cells were pre-treated with anti-CD81 monoclonal antibody or control mouse IgG at 1 h before infection. Cells were then infected with J6/JFH1/Luc reporter viruses for 6 h. At 48 h post-infection, the cells were lysed and assayed for luciferase activity. Activities are expressed as the relative activity compared to that of the null antibody-treated sample. The assays were repeated at least three times, and the mean values are presented.

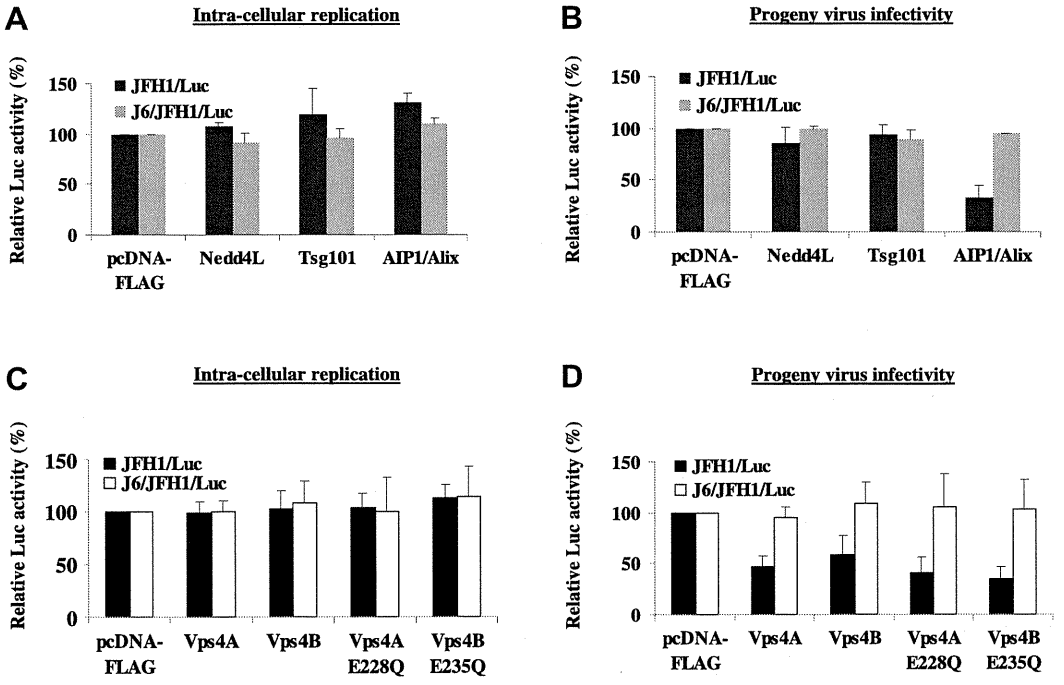

Fig. 4. Effect of ESCRT family protein expression on intra-cellular replication and progeny virus production in Huh7.5 cells. Huh7.5 cells were electroporated with JFH1/Luc and J6/JFH1/Luc RNA, respectively. The RNA-electroporated cells were then transfected with ESCRT protein expression plasmids. At 96 h after transfection, the culture supernatants were collected, and the cells were harvested. (A, C) Cell lysates were assayed for luciferase activity to assess intra-cellular virus replication. (B, D) Collected supernatants were added to naïve Huh7.5 cells and incubated for 48 h, and then the luciferase activity of the cells was analyzed to assess progeny virus infectivity. The data relative to that of luciferase activity in the absence of ESCRT protein (pcDNA-FLAG) is indicated. The assays were repeated at least three times, and the mean and standard error are presented.

replication and virus production were analyzed by monitoring the luciferase activity of reporter RNA-transfected cells (Fig. 4A), and the luciferase activity expressed by supernatant virus (Fig. 4B). As shown in Fig. 4A, the overexpression of Nedd4L, Tsg101, and AIP/Alix had no effect on the intra-cellular replication of either reporter HCV. As shown in Fig. 4B, the virus production from J6/JFH1/Luc also was not affected by these ESCRT protein expressions. In contrast, the expression of AIP/Alix decreased the virus production from JFH1/Luc by 50%. This result implied that the ESCRT machinery might have played some role in the difference in the efficacy of virus production observed between JFH1 and J6/JFH1. AAA-ATPase Vps4, which is present in humans in two isoforms (Vps4A and Vps4B), is a key modulator protein for the final step of ESCRT machinery. To analyze the role of ESCRT in HCV virus production, we constructed expression vectors for Vps4A and 4B, as well as expression vectors for a dominant-negative Vps4A(E228Q) and Vps4B(E235Q) [19]. As shown in Fig. 4C, the intra-cellular replications of JFH1 and J6/JFH1 were not influenced by the wild-type or dominant-negative Vps4 expression. In contrast, the levels of virus production of JFH1/Luc were reduced up to 50% by the expression of both dominant-negative Vps4 mutants (Fig. 4D). Interestingly, neither dominant-negative Vps4 influenced the virus production of J6/JFH1/Luc. These results implied that JFH1 might utilize the ESCRT machinery for release of infectious virus particles.

3.5. Effect of polyions on the infectivity of the J6/JFH1/Luc reporter virus

Next, we tested the usefulness of the J6/JFH1/luc reporter system for virus entry analysis. The binding of the viral and cellular receptors is coordinated with the ionic conditions, indicating that compounds that affect the ionic charge of the receptor surface might be potent inhibitors of virus infection [21,22]. Polyions with a positive or negative charge are frequently used for virus entry analyses, and exhibit inhibitory activity on virus infection [21,22]. Therefore, we investigated the effect of different polyions on the infectivity of the J6/JFH1/Luc virus in order to clarify the influence of electrostatic interactions in virus binding to cell membranes. As candidate compounds, we used both polymers having a positive charge (polybrene (size of 3000 Da), DEAE-dextran (100,000 Da), and poly-L-lysine (500,000 Da)) and those having a negative charge (heparin (15,000 Da), dextran sulfate (50,000 Da), and polyvinyl sulfate (150,000 Da)). These polymers were added to the Huh7.5 cells at 1 h before inoculation of the J6/JFH1/Luc virus into the cells. After 48 h of inoculation, the cells were harvested and the luciferase activity was analyzed (Fig. 5A and B). As shown in Fig. 5A, two polyanions, heparin and polyvinyl sulfate, decreased the infectivity of J6/JFH1/Luc virus in a dose-dependent manner, whereas one polyanion, dextran sulfate, enhanced the infectivity up to 2-fold. In the case of polycations, the addition of polybrene enhanced virus

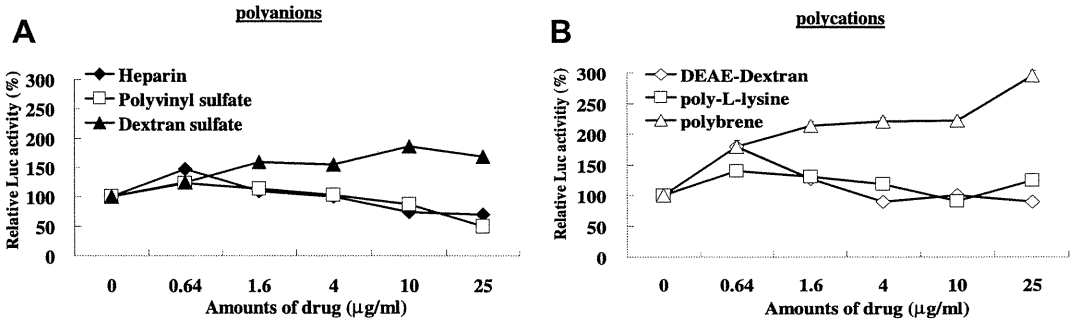

Fig. 5. Effect of multiple polyions on J6/JFH1/Luc virus infection of Huh7.5 cells. Huh7.5 cells were infected with J6/JFH1/Luc virus in the presence of each of the polyions for 6 h, and a luciferase assay was performed 48 h later. The data was expressed as the relative activity compared to the luciferase activity in the absence of polyions. The assays were repeated at least three times, and the mean values are presented.

infection up to 3-fold in a dose-dependent manner, although poly-L-lysine and DEAE-dextran showed no effect on the infectivity of the J6/JFH1/Luc virus (Fig. 5B). The effect shown by compounds belonging to positive and negative polyions suggested that the electric charge is not sufficient by itself to explain the inhibitory or enhancing activity of these drugs on the HCV virus entry. These results indicated that the J6/JFH1/Luc virus was useful to easily monitor HCV virus entry.

3.6. Screening of microRNA inhibition on intra-cellular HCV replication

To confirm the usefulness of the J6/JFH1/Luc reporter system in the analysis targeting intra-cellular replication of HCV, we analyzed the possible involvement of micro RNAs (miRNAs) in HCV infection. miRNAs are evolutionarily conserved, small, non-coding RNA molecules that regulate gene expression at the level of translation [23,24]. Recently, it has been reported that some miRNAs influence the replication of HCV in the cells [25–27]. For example, the expression of miR-122 in the cells might be essential for HCV replication [25]. In addition, the number of miRNAs has been increasing due to numerous strenuous analyses in recent years. Therefore, we compared the full sequences of the viral genome among 4 different HCV strains (H77C, Con1, J6, JFH1) with the sequences of 630 human miRNAs using the miRNA database program (RegRNA: http://regrna.mbc.nctu.edu.tw/index.php), and then identified 54 miRNAs that matched with at least one HCV strain. 10 of the 54 miRNAs matched with all four HCV strains. Hence, we focused on analysis of the function of the 10 miRNAs on HCV replication and prepared commercially available miRNA inhibitors (Anti-miR™ miRNA inhibitor, Ambion) that were chemically modified, single-stranded nucleic acids designed to specifically bind to and inhibit endogenous target miRNA molecules. The J6/JFH1/Luc RNA-electroporated cells were transfected with each of the 10 specific miRNA inhibitors and the luciferase activities were analyzed at 48 h post-transfection of the inhibitors. None of the miRNA inhibitors significantly affected the cell viability (data not shown). As shown in Fig. 6A, the inhibition of miR-122 reduced the level of intra-cellular virus replication by up to 50% as previously reported [25]. A similar reduction of viral replication was also observed by treatment with the miR-34b inhibitor. The treatment with an anti-miR negative control that is a random sequence anti-miR molecules that has been extensively tested in human cell lines and validated to not produce identifiable effects on known miRNA functions showed no significant effect on HCV replication. None of the other inhibitors showed any significantly greater effect on the

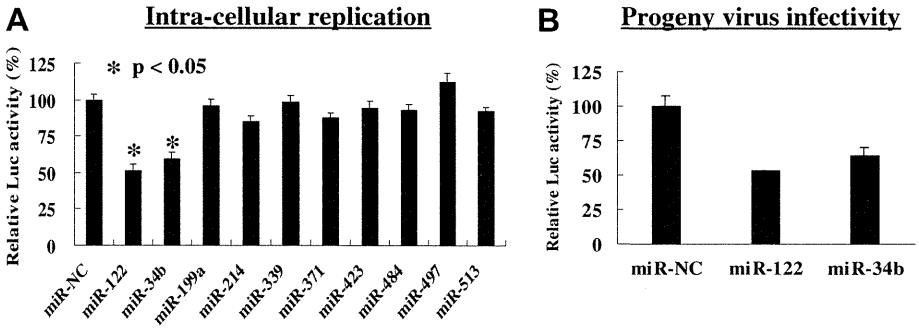

Fig. 6. Effect of miRNA inhibitor on intra-cellular replication of J6/JFH1/Luc RNA in Huh7.5 cells. Target cells were electroporated with J6/JFH1/Luc RNA, and then transfected with a miRNA-specific or a non-target negative control miRNA inhibitor. At 48 h post-transfection, cells were harvested and analyzed for luciferase activity (A). In parallel, the culture supernatants were collected at 48 h post-transfection to assess the effect of miRNA inhibitors on the virus production. The supernatants were added to naïve Huh7.5 cells, and the progeny virus infectivities were then analyzed by luciferase assay. (B) The data relative to the luciferase activity obtained from a non-target negative control miRNA inhibitor are indicated. The assays were repeated at least three times, and the mean and standard error are presented. Statistical significance relative to the negative control miRNA samples as calculated by *t*-test is shown (*$p < 0.05$).

virus replication than the anti-miR negative control. The miR-34b and miR-122 inhibitors decreased the virus production to the levels 64% and 53% of the control, respectively (Fig. 6B). Since the extent of the reduction in virus production was comparable with that of intra-cellular HCV RNA levels (Fig. 6A), it was likely that these miRNA inhibitors affected the intra-cellular viral replication rather than interfering with the particle formation and the release of the virion. These results suggest that the function of miR-34b could affect the replication of HCV, and also suggested that the J6/JFH1/Luc system was useful to analyze the intra-cellular replication of HCV.

4. Discussion

In this report, we generated two bicistronic luciferase reporter HCV clones from JFH1 and J6/JFH1, and established a unifying system that can monitor intra-cellular viral replication, virion production, and virus entry. Using two constructs, we initially compared the potential of intra-cellular viral replication and virus production. After transfection of reporter RNAs, the level of the intra-cellular core protein and the luciferase activity in RNA-transfected cells showed similar kinetics for JFH1/Luc and J6/JFH1/Luc (Fig. 1B and C). In contrast, both the efficacy of core protein production into the culture supernatant and the infectivity of supernatant virus from J6/JFH1/Luc were significantly higher than that of JFH1/Luc (Fig. 2A and B). These results indicated two possibilities that JFH1 and J6/JFH1 utilize different machinery for progeny virus packaging and budding, or that they utilize the same machinery for the virus production but to a different degree. To evaluate the difference in the virus production between JFH1 and J6/JFH1, we analyzed the role of ESCRT machinery in virus production (Fig. 4A–D). Dominant-negative Vps4 expression inhibited JFH1/Luc virus production, but did not influence J6/JFH1/Luc virus production. In the course of preparing this manuscript, Corless et al. reported that HCV requires late components of the ESCRT pathway for release of infectious virus particles [28]. They showed that a dominant-negative Vps4 expression inhibited the production of virus-like particles derived from JFH1 in a dose-dependent manner. The findings reported by Corless et al. and the findings of our present study emphasize that the ESCRT machinery plays an essential role in JFH1 virus production.

To examine the virus entry, we analyzed the effect of anti-CD81 antibody and polyions on reporter virus infectivity (Figs. 3B and 5A and B). The pre-treatment with anti-CD81 antibody decreased the infectivity of the reporter J6/JFH virus in a dose-dependent manner. The result suggested that the reporter J6/JFH1 virus, similar to HCVcc, utilized the CD81 as a major entry receptor, and that our reporter virus could be used as a surrogate model of HCV entry analysis. As a result of polyions analysis, one of the polycations (dextran sulfate) and one of the polyanions (polybrene) increased the reporter virus infectivity, and the remainder of the polyions inhibited the virus infectivity. These results indicate the possibility that not only the electrostatic condition of polyions but also their molecular weight may be a determinant of the receptor binding of HCV. Considering that several membrane molecules have been identified as candidate cellular receptors for HCV entry [15,29,30], the polyions could interact with a different molecule(s) to influence virus production. As for heparin, it was reported that cell surface heparan sulfate proteoglycans play an important role in mediating HCV envelope–target cell interaction [31]. Basu et al. [32] also reported that heparin treatment completely blocked HIV/HCV E1-E2 pseudotype infection. In their analysis, however, the inhibitory effect of heparin against cell culture-grown HCV H77 was somewhat lower than that of HIV/HCV E1-E2 pseudotypes. In our present study, the level of inhibitory effect of heparin on J6/JFH1 reporter virus infection was not so prominent. Collectively, these data suggest a possibility that cell surface heparan sulfate proteoglycans contribute to the infection of both HIV/HCV E1–E2 pseudotype and cell culture-grown HCV with a different degree. Therefore, to develop a polyion-based anti-HCV drug, a more detailed assessment of the interaction between each candidate receptor and polyion is necessary.

Using microRNA inhibitors, the decrease of miR-34b expression suppressed intra-cellular HCV replication (Fig. 6A). miR-34b belongs to the evolutionary conserved microRNA family of miR-34s [33], known for their role in the p53 tumor suppressor network [34]. miR-34s have been shown to be controlled in a tissue-specific manner by p53. Both wild-type and mutant-type p53 protein expressions in serum and cytoplasm of liver tissue were more pronounced in patients with hepatocellular carcinoma associated with HCV infection [35]. Wild-type p53 binds to a transcriptional regulatory element of miR-34s, thereby up-regulating miR-34 expression [34]. However, it is not understood whether the mutant-type p53 increases miR-34b expression. Furthermore, HCV replication in chronic hepatitis is higher than that of hepatocellular carcinoma [36]. Therefore, more detailed research is needed to reveal the significance of miR-34b expression in HCV replication and hepatocellular carcinoma.

As mentioned above, we have generated a recombinant luciferase reporter HCV, and have shown that the reporter HCV could be used for the quantitative analyses of intra-cellular replication, virus entry, and virion production. In general, the intra-cellular HCV replication has been analyzed by the quantitative real-time RT-PCR method that could detect a small amount of viral RNA because of the greatly high sensitivity. However, the real-time RT-PCR method involves multi-step procedures of the RNA extraction, the reverse transcription and the PCR reaction, which require skillfulness to perform. The high sensitivity and the multiple-steps of the real-time RT-PCR system sometimes cause an experimental error(s) when conducted by less-experienced individuals. On the other hand, our HCV luciferase reporter system is simpler and easier to perform compared to the real-time PCR system. The significant advantage of the reporter HCV is that it can analyze a large number of samples at a time in a time- and cost-saving manner. Also, it can be used to evaluate all the

events of viral life cycle. By using it, we have started the screening of anti-HCV substances from the natural resource chemical libraries and found a number of potential candidates for the analysis. Thus, this system can be applicable for robust screening analyses of chemical compounds to discover a potential therapeutic target of HCV.

Acknowledgments

The authors are grateful to Dr C.M. Rice (Center for the Study of Hepatitis C, the Rockefeller University, New York, NY, USA) for providing pFL-J6/JFH1 and Huh7.5 cells. We also thank the members of our department for their helpful discussion. This study was supported in part by Health and Labour Sciences Research Grants from the Ministry of Health, Labour and Welfare, Japan, and a SATREPS Grant from Japan Science and Technology Agency (JST) and Japan International Cooperation Agency (JICA). This study was also carried out as part of Japan Initiative for Global Research Network on Infectious Diseases (J-GRID), Ministry of Education, Culture, Sports, Science and Technology, and the Global Center of Excellence (G-COE) Program at Kobe University Graduate School of Medicine.

References

[1] T.L. Tellinghuisen, M.J. Evans, T. von Hahn, S. You, C.M. Rice, Studying hepatitis C virus: making the best of a bad virus, J. Virol. 81 (2007) 8853–8867.

[2] N. Kato, M. Hijikata, Y. Ootsuyama, M. Nakagawa, S. Ohkoshi, T. Sugimura, K. Shimotohno, Molecular cloning of the human hepatitis C virus genome from Japanese patients with non-A, non-B hepatitis, Proc. Natl. Acad. Sci. U.S.A. 87 (1990) 9524–9528.

[3] S. Chevaliez, J.M. Pawlotsky, Hepatitis C virus: virology, diagnosis and management of antiviral therapy, World J. Gastroenterol. 13 (2007) 2461–2466.

[4] M. Laguno, C. Cifuentes, J. Murillas, S. Veloso, M. Larrousse, A. Payeras, L. Bonet, F. Vidal, A. Milinkovic, A. Bassa, C. Villalonga, I. Perez, C. Tural, M. Martinez-Rebollar, M. Calvo, J.L. Blanco, E. Martinez, J.M. Sanchez-Tapias, J.M. Gatell, J. Mallolas, Randomized trial comparing pegylated interferon alpha-2b versus pegylated interferon alpha-2a, both plus ribavirin, to treat chronic hepatitis C in human immunodeficiency virus patients, Hepatology 49 (2009) 22–31.

[5] A. El-Shamy, M. Nagano-Fujii, N. Sasase, S. Imoto, S.R. Kim, H. Hotta, Sequence variation in hepatitis C virus nonstructural protein 5A predicts clinical outcome of pegylated interferon/ribavirin combination therapy, Hepatology 48 (2008) 38–47.

[6] D.P. Webster, P. Klenerman, J. Collier, K.J. Jeffery, Development of novel treatments for hepatitis C, Lancet Infect. Dis. 9 (2009) 108–117.

[7] P.J. Lukavsky, Structure and function of HCV IRES domains, Virus. Res. 139 (2009) 166–171.

[8] V. Lohmann, F. Korner, J. Koch, U. Herian, L. Theilmann, R. Bartenschlager, Replication of subgenomic hepatitis C virus RNAs in a hepatoma cell line, Science 285 (1999) 110–113.

[9] T. Wakita, T. Pietschmann, T. Kato, T. Date, M. Miyamoto, Z. Zhao, K. Murthy, A. Habermann, H.G. Krausslich, M. Mizokami, R. Bartenschlager, T.J. Liang, Production of infectious hepatitis C virus in tissue culture from a cloned viral genome, Nat. Med. 11 (2005) 791–796.

[10] B.D. Lindenbach, M.J. Evans, A.J. Syder, B. Wolk, T.L. Tellinghuisen, C.C. Liu, T. Maruyama, R.O. Hynes, D.R. Burton, J.A. McKeating, C. M. Rice, Complete replication of hepatitis C virus in cell culture, Science 309 (2005) 623–626.

[11] T. Kato, T. Date, M. Miyamoto, M. Sugiyama, Y. Tanaka, E. Orito, T. Ohno, K. Sugihara, I. Hasegawa, K. Fujiwara, K. Ito, A. Ozasa, M. Mizokami, T. Wakita, Detection of anti-hepatitis C virus effects of interferon and ribavirin by a sensitive replicon system, J. Clin. Microbiol. 43 (2005) 5679–5684.

[12] L. Deng, T. Adachi, K. Kitayama, Y. Bungyoku, S. Kitazawa, S. Ishido, I. Shoji, H. Hotta, Hepatitis C virus infection induces apoptosis through a Bax-triggered, mitochondrion-mediated, caspase 3-dependent pathway, J. Virol. 82 (2008) 10375–10385.

[13] K. Kamada, T. Igarashi, M.A. Martin, B. Khamsri, K. Hatcho, T. Yamashita, M. Fujita, T. Uchiyama, A. Adachi, Generation of HIV-1 derivatives that productively infect macaque monkey lymphoid cells, Proc. Natl. Acad. Sci. U.S.A. 103 (2006) 16959–16964.

[14] T. Schaller, N. Appel, G. Koutsoudakis, S. Kallis, V. Lohmann, T. Pietschmann, R. Bartenschlager, Analysis of hepatitis C virus superinfection exclusion by using novel fluorochrome gene-tagged viral genomes, J. Virol. 81 (2007) 4591–4603.

[15] P. Pileri, Y. Uematsu, S. Campagnoli, G. Galli, F. Falugi, R. Petracca, A. J. Weiner, M. Houghton, D. Rosa, G. Grandi, S. Abrignani, Binding of hepatitis C virus to CD81, Science 282 (1998) 938–941.

[16] A. Calistri, C. Salata, C. Parolin, G. Palu, Role of multivesicular bodies and their components in the egress of enveloped RNA viruses, Rev. Med. Virol. 19 (2009) 31–45.

[17] S. Welsch, B. Muller, H.G. Krausslich, More than one door – budding of enveloped viruses through cellular membranes, FEBS Lett. 581 (2007) 2089–2097.

[18] B. Strack, A. Calistri, S. Craig, E. Popova, H.G. Gottlinger, AIP1/ALIX is a binding partner for HIV-1 p6 and EIAV p9 functioning in virus budding, Cell 114 (2003) 689–699.

[19] P.D. Bieniasz, Late budding domains and host proteins in enveloped virus release, Virology 344 (2006) 55–63.

[20] J.H. Hurley, P.I. Hanson, Membrane budding and scission by the ESCRT machinery: it's all in the neck, Nat. Rev. Mol. Cell Biol. 11 (2010) 556–566.

[21] O. Bagasra, P. Whittle, B. Heins, R.J. Pomerantz, Anti-human immunodeficiency virus type 1 activity of sulfated monosaccharides: comparison with sulfated polysaccharides and other polyions, J. Infect. Dis. 164 (1991) 1082–1090.

[22] J. Haldar, D. An, L. Alvarez de Cienfuegos, J. Chen, A.M. Klibanov, Polymeric coatings that inactivate both influenza virus and pathogenic bacteria, Proc. Natl. Acad. Sci. U.S.A. 103 (2006) 17667–17671.

[23] A. Ventura, T. Jacks, microRNAs and cancer: short RNAs go a long way, Cell 136 (2009) 586–591.

[24] D.P. Bartel, microRNAs: target recognition and regulatory functions, Cell 136 (2009) 215–233.

[25] C.L. Jopling, M. Yi, A.M. Lancaster, S.M. Lemon, P. Sarnow, Modulation of hepatitis C virus RNA abundance by a liver-specific microRNA, Science 309 (2005) 1577–1581.

[26] G. Randall, M. Panis, J.D. Cooper, T.L. Tellinghuisen, K.E. Sukhodolets, S. Pfeffer, M. Landthaler, P. Landgraf, S. Kan, B.D. Lindenbach, M. Chien, D.B. Weir, J.J. Russo, J. Ju, M.J. Brownstein, R. Sheridan, C. Sander, M. Zavolan, T. Tuschl, C.M. Rice, Cellular cofactors affecting hepatitis C virus infection and replication, Proc. Natl. Acad. Sci. U.S.A. 104 (2007) 12884–12889.

[27] Y. Murakami, H.H. Aly, A. Tajima, I. Inoue, K. Shimotohno, Regulation of the hepatitis C virus genome replication by miR-199a, J. Hepatol. 50 (2009) 453–460.

[28] L. Corless, C.M. Crump, S.D. Griffin, M. Harris, Vps4 and the ESCRT-III complex are required for the release of infectious hepatitis C virus particles, J. Gen. Virol. 91 (2010) 362–372.

[29] A. Ploss, M.J. Evans, V.A. Gaysinskaya, M. Panis, H. You, Y.P. de Jong, C.M. Rice, Human occludin is a hepatitis C virus entry factor required for infection of mouse cells, Nature 457 (2009) 882–886.

[30] M.J. Evans, T. von Hahn, D.M. Tscherne, A.J. Syder, M. Panis, B. Wolk, T. Hatziioannou, J.A. McKeating, P.D. Bieniasz, C.M. Rice, Claudin-1 is a hepatitis C virus co-receptor required for a late step in entry, Nature 446 (2007) 801–805.

[31] H. Barth, C. Schafer, M.I. Adah, F. Zhang, R.J. Linhardt, H. Toyoda, A. Kinoshita-Toyoda, T. Toida, T.H. Van Kuppevelt, E. Depla, F. Von Weizsacker, H.E. Blum, T.F. Baumert, Cellular binding of hepatitis C virus envelope glycoprotein E2 requires cell surface heparan sulfate, J. Biol. Chem. 278 (2003) 41003–41012.

[32] A. Basu, T. Kanda, A. Beyene, K. Saito, K. Meyer, R. Ray, Sulfated homologues of heparin inhibit hepatitis C virus entry into mammalian cells, J. Virol. 81 (2007) 3933–3941.

[33] M. Fabbri, C.M. Croce, G.A. Calin, microRNAs, Cancer J. 14 (2008) 1–6.

[34] L. He, X. He, S.W. Lowe, G.J. Hannon, microRNAs join the p53 network – another piece in the tumour-suppression puzzle, Nat. Rev. Cancer 7 (2007) 819–822.

[35] A.M. Attallah, G.E. Shiha, H. Ismail, S.E. Mansy, R. El-Sherbiny, I. El-Dosoky, Expression of p53 protein in liver and sera of patients with liver fibrosis, liver cirrhosis or hepatocellular carcinoma associated with chronic HCV infection, Clin. Biochem. 42 (2009) 455–461.

[36] M. Colombo, Natural history and pathogenesis of hepatitis C virus related hepatocellular carcinoma, J. Hepatol. 31 (Suppl. 1) (1999) 25–30.